AD-A032 263 VON KARMAN INST FOR FLUID DYNAMICS RHODE-SAINT-GENESE--ETC F/G 20/4
FILM COOLED SMALL TURBINE BLADE RESEARCH. VOLUME II. FILM COOLI--ETC(U)
JUN 76 B E RICHARDS, J P VILLE, C APPELS DA-ERO-75-G-074

UNCLASSIFIED NL

1 OF 1
AD A032 263

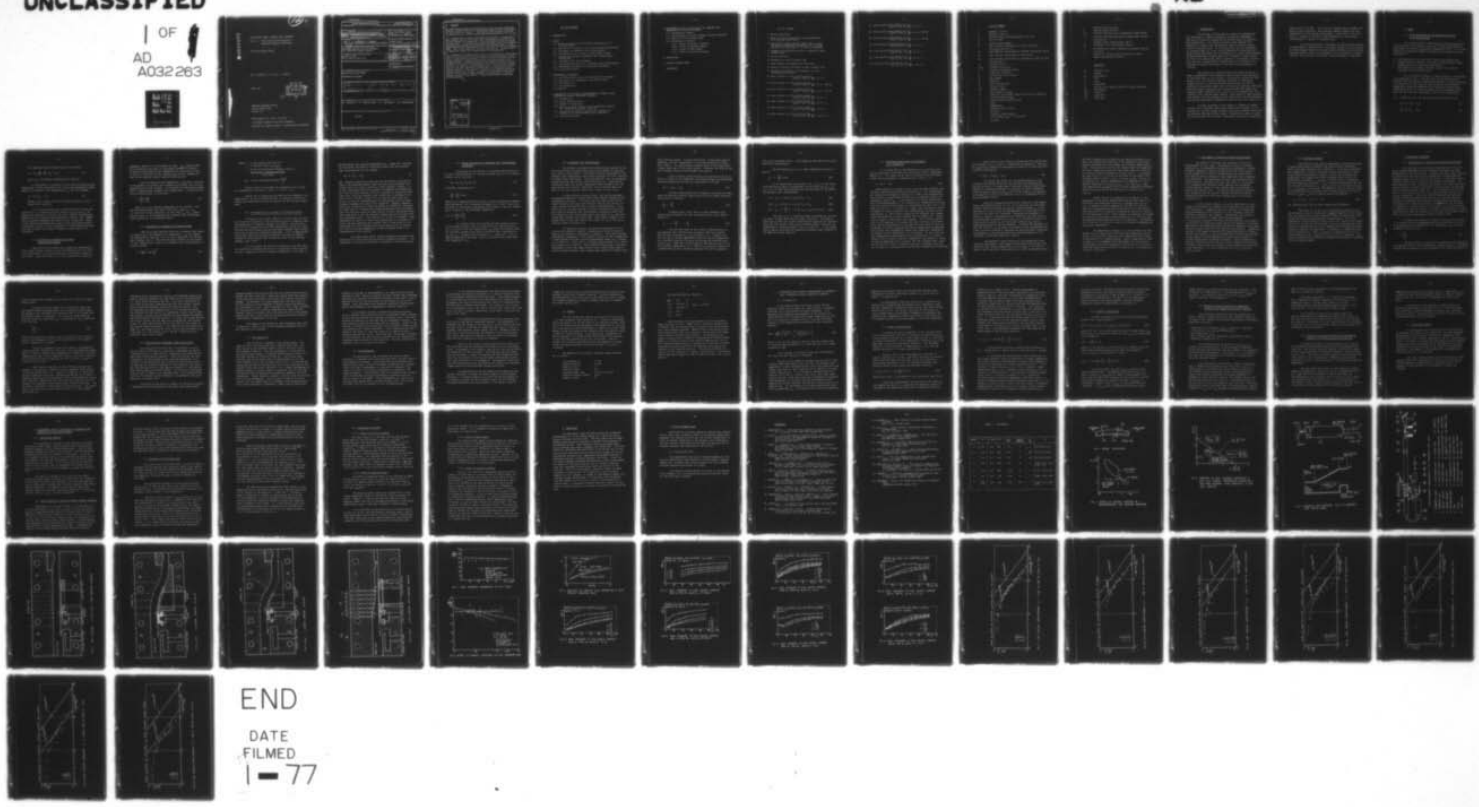

END

DATE FILMED
1-77

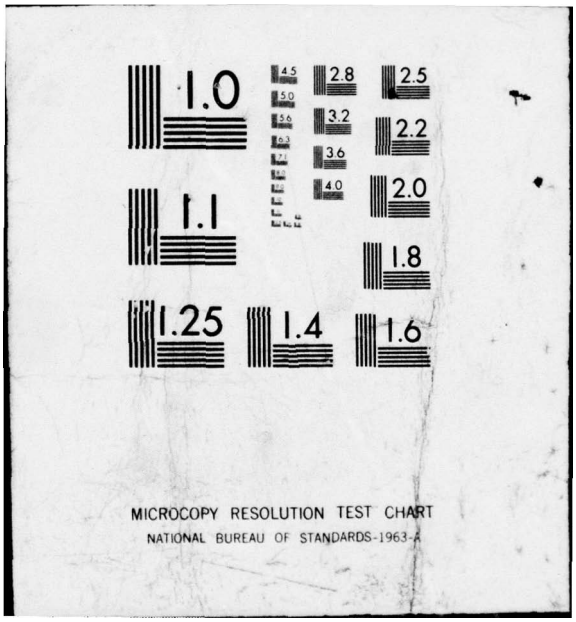
1.0
1.1
1.25
1.4
1.6
1.8
2.0
2.2
2.5
2.8
3.2
3.6
4.0
4.5
5.0
5.6
6.3
MICROCOPY RESOLUTION TEST CHART
NATIONAL BUREAU OF STANDARDS-1963-A

FILM COOLED SMALL TURBINE BLADE RESEARCH

Vol. II - FILM COOLING EFFECTIVENESS AT SIMULATED TURBINE CONDITIONS

1st Year Annual Report

B.E. RICHARDS, J.P. VILLE, C. APPELS

JUNE 1976

EUROPEAN RESEARCH OFFICE
United States Army
London, U.K.

Grant Number DA - ERO - 75-G-074
von Karman Institute for Fluid Dynamics

UNCLASSIFIED

SECURITY CLASSIFICATION OF THIS PAGE (When Data Entered)

REPORT DOCUMENTATION PAGE

READ INSTRUCTIONS BEFORE COMPLETING FORM

1. REPORT NUMBER

2. GOVT ACCESSION NO.

3. RECIPIENT'S CATALOG NUMBER

4. TITLE (and Subtitle)

FILM COOLED SMALL TURBINE BLADE RESEARCH. Volume II
~~PART I: AERODYNAMIC STUDY OF SECONDARY FLOWS~~
PART II: FILM COOLING EFFECTIVENESS AT SIMULATED TURBINE CONDITIONS

5. TYPE OF REPORT & PERIOD COVERED

1st YEAR ANNUAL REPORT
DEC 75 - JUNE 76

6. PERFORMING ORG. REPORT NUMBER

7. AUTHOR(s)

PART I: C. SIEVERDING & P. MARCHAL
PART II: B. E. RICHARDS, J.P. VILLE & C. APPELS

8. CONTRACT OR GRANT NUMBER(s)

DAERO-75-074
DA-ERO-75-G-074

9. PERFORMING ORGANIZATION NAME AND ADDRESS

VON KARMAN INSTITUTE FOR FLUID DYNAMICS
1640, RHODE-SAINT-GENESE, BELGIUM

10. PROGRAM ELEMENT, PROJECT, TASK AREA & WORK UNIT NUMBERS

61102A-1T161102B35E-00-530

11. CONTROLLING OFFICE NAME AND ADDRESS

USA R&S GP (EUR)
BOX 65, FPO NEW YORK 09510

12. REPORT DATE

JUNE 1976

13. NUMBER OF PAGES

PART I: 81 PART II: 67p.

14. MONITORING AGENCY NAME & ADDRESS (if different from Controlling Office)

15. SECURITY CLASS. (of this report)

UNCLASSIFIED

15a. DECLASSIFICATION/DOWNGRADING SCHEDULE

16. DISTRIBUTION STATEMENT (of this Report)

APPROVED FOR PUBLIC RELASE

DISTRIBUTION UNLIMITED

17. DISTRIBUTION STATEMENT (of the abstract entered in Block 20, if different from Report)

Annual rept. no. 1 for period ending Jun 76

18. SUPPLEMENTARY NOTES

19. KEY WORDS (Continue on reverse side if necessary and identify by block number)

(U) PROPULSION (U) INTERNAL FLOWS (U) FILM COOLING (U) CASCADE FLOWS

20. ABSTRACT (Continue on reverse side if necessary and identify by block number)

SEE OVER

DD FORM 1 JAN 73 1473 EDITION OF 1 NOV 65 IS OBSOLETE

UNCLASSIFIED

SECURITY CLASSIFICATION OF THIS PAGE (When Data Entered)

367 475

6pg

20. ABSTRACT

The overall study concerns an investigation on the cooling and aerodynamic problems associated with a high speed turbine cascade of small blade height for use on small gas turbines. The secondary flow behavior in turbines is presented in Vol. I and the cooling aspects are presented in Vol. II.

Vol. I reports on the study of small aspect ratio blades. A program has been initiated with the aim of obtaining a better physical understanding of the real secondary flow phenomenon. The total program will cover a period of three years. It includes very detailed low speed tests with measurements inside the blade passage, cross checking of the low speed tests in a high speed cascade and the investigation of the effect of film cooling on secondary flows. Vol I, which reports on the first year efforts, presents mainly low speed test results and a limited amount of high speed data.

Vol. II reports on the first year efforts on the measurement of effectiveness of a film cooling system for a small turbine by injection through inclined holes. A short duration facility was used to provide isothermal wall data at flow conditions carefully selected to simulate those expected in an advanced turbine. Appropriate heat and mass transfer equations have been developed to illustrate the interpretation and usefulness of data obtained in this as yet relatively unconventional method. The measurements showed: that there are small increases in effectiveness for injection on convex surfaces compared to flat surfaces; a change in flow Reynolds number only slightly changes effectiveness; a lowering of the mainstream Mach number from 0.6 to 0.3 causes a sizable decrease in effectiveness; a pressure gradient, typical of that seen on a turbine also decreases considerably the effectiveness.

LIST OF CONTENTS

LIST OF FIGURES

LIST OF SYMBOLS

a	exponent in eq. 6
b	exponent in eq. 6
c	specific heat of backing material (eq. 23)
c_f	skin friction
d	coolant hole diameter
h	heat transfer coefficient of film in terms of $(T_{rm}-T_{wo})$ {see eq. 11}
h_c	heat transfer coefficient of internal convection (eq.2)
h_f	heat transfer coefficient of film (eq.3)
h_o	heat transfer coefficient on outside wall with no film cooling (eq.1)
k	constant in eq.6
k, k_w	conductivity of wall
K	frequency parameter (eq.24)
l	blade wall thickness
m	coolant mass ratio (eq.6)
M	Mach number
p	pressure
q	heat transfer rate
R	radius of wall
Re	Reynolds number
s	slot height (in eq.6)
s'	effective slot height (sum of the area of injection holes divided by span)
S	scaling factor given by eq.21
t	time
T	temperature
T	periodic time in eq.24
u	velocity
x	distance along surface
$\bar{x}$	$(x/ms')(Re_c\mu_c/\mu_m)^{-0.25}$ from eq.6
y	distance

α	function given by eq.28
β	function given by eq.27
ΔT_1	constant defining size of temperature ramp (eq.25)
ΔT_2	constant defining amplitude of temperature fluctuation (eq.25)
η	adiabatic wall effectiveness (eq.5)
η_q	isothermal wall effectiveness (eq.13)
Θ	non-dimension coolant temperature parameter (eq.10)
μ	viscosity
ρ	density of fluid or backing material in eq.23
τ	dummy time parameter (eq.23)

SUBSCRIPTS

aw	adiabatic wall
c	coolant
ex	experimental
f	film
i	inner
m	mainstream
o	hot-gas side, supply condition or mean condition
op	operational
ref	recovery
wo	outer wall
wi	inner wall

1. INTRODUCTION

Film cooling is being used as a means of supplementing the techniques of internal convection cooling and impingement cooling to increase the capability of turbine blades to withstand high temperatures. For reasons of mainly blade strength the injection of coolant into the boundary layer is usually through series of inclined holes. In the region near the wall downstream of injection when the "film" is most effective in protecting the blade surface from heat, the flow behaviour is in this case dominated by three-dimensional effects mainly of a turbulent viscous nature. The flow is so complicated that at present it is necessary to place most reliance on experiments to enable empirical relations to be developed to predict the effect of the flow on the parameters of interest.

The majority of research studies have been carried out under incompressible flow situations (Ref.1) and a large proportion of these have been on slot cooling. Such studies provide the fundamental basis for prediction methods, empirical or otherwise, however accuracy in calculating real turbine flows can only be expected to be achieved under more realistically simulated conditions. Blow down tunnels have been used to provide both Mach number and Reynolds number simulation (e.g., Ref.2), but the temperature field simulation has sometimes been ignored. More recently, short duration wind tunnels have been applied to the turbine film cooling problem to provide more appropriate temperature field scaling (e.g., Refs.3,4).

The work described in this report is related to studies carried out in a piston driven short duration wind tunnel on film cooling of a surface through inclined holes which resemble those used on projected advanced turbine blades. Attention was given to carrying out the tests at M, Re and T conditions realistically simulating

those found in turbines. The aim of the research was to examine the effect of wall curvature, Mach numbers, Reynolds number and flow temperature on film cooling effectiveness. This study is the first part of a larger one leading to the measurement of film cooling effectiveness in regions of secondary flow.

The following chapter is devoted to a more detailed account of experimental simulation of a film cooled surface in a gas turbine. The third chapter explains the experimental equipment and techniques, the experimental results are presented in the following two chapters. Finally, the conclusions and future planned programme is presented.

2. THEORY

2.1. Brief description of the design calculation of a cooling system

In a turbine cooling system design an energy balance must be carried out on the blade to arrive at a cooling configuration which meets the required blade metal temperature limit. For a blade cooled by a convection system the analysis can be broken up into three parts :

1. The prediction of the heat flux from the hot exterior gas ;
2. A heat conduction analysis to provide a detailed map of metal temperatures for blade-stress predictions ;
3. The prediction of complex internal coolant flow paths for convection cooling calculations.

For illustration purposes a simplification of the problem is illustrated in Fig.1. The heat flux to the blade from the exterior flow and from the blade to the coolant is usually expressed as a product of a heat transfer coefficient and the difference between the adiabatic temperature (or recovery or effective gas temperature, which for subsonic speeds can be considered nearly equal to the flow total temperature) and the wall temperature.

i.e. respectively for the hot-gas-side and the coolant side :

$$q_o = h_o \, (T_{rm} - T_{\omega o}) \qquad (1)$$

$$q_c = h_c \, (T_{\omega i} - T_{rc}) \qquad (2)$$

The temperature drop through the wall is given by :

$$q = - k_\omega \frac{dT}{dy} = \frac{k_\omega}{\ell} (T_{\omega o} - T_{\omega i}) \qquad (3)$$

where k_ω is the thermal conductivity of the wall.

If the surface is cooled by a film, then the effective gas temperature is often indicated to be a local film temperature (often known as the adiabatic wall temperature), $T_{a\omega}$ and Eq.1 becomes :

$$q_f = h_f (T_{a\omega} - T_{\omega o}) \qquad (4)$$

where h_f has a value not too far different from h_o in Eq.1 except near injection.

In a practical design for a given blade profile and test conditions, it is required to alter values of h_c, h_f and $T_{a\omega}$ by appropriate selection of coolant flow rate, internal blade passage geometry and film injection part geometry to achieve a wall temperature variation throughout the blade as small as possible. Hence in the iterative procedure that ensues in any such energy balance calculation a useful initial assumption for calculating the hot-gas-side flow to which this study is devoted, is that the wall is isothermal.

2.2. Definition of adiabatic wall film cooling effectiveness

Many film cooling studies have treated the determination of the heat transfer coefficient and film adiabatic wall (or local film) temperature distribution separately with primary interest on the latter, since the value of h_f is less sensitive to injection

parameters. More will be said about h_f later. $T_{a\omega}$, however, does vary considerably and hence is the harder parameter to predict. In addition the adiabatic wall temperature is significant in that it gives an indication of the limiting value of wall temperature that can be attained without internal blade cooling.

The film adiabatic wall temperature is not only a function of the geometry and primary and secondary flow fields, but also the temperature of the gas streams. To eliminate the temperature dependence, a dimensionless adiabatic wall temperature, η, called the film cooling effectiveness is often used :

$$\eta = \frac{T_{rm} - T_{a\omega}}{T_{rm} - T_{rc}} \qquad (5)$$

where T_{rc} is the recovery temperature of the coolant. Film cooling effectiveness then varies from unity, when $T_{a\omega} = T_{rc}$ i.e. the film is fully effective, to zero, when $T_{a\omega} = T_{rm}$ which usually occurs so far downstream from injection that the boundary layer recovers to its undisturbed value.

2.3. Assessment of adiabatic wall effectiveness

There exist many theories which use a boundary layer model to estimate the film adiabatic wall temperature. $T_{a\omega}$ for regions far downstream of injection (e.g. for slot injection, see Stollery and El Ehwany, Ref.5). Then the following relation for the adiabatic wall temperature in terms of an adiabatic wall effectiveness is usually derived :

$$\eta = k\left(\frac{x}{ms}\right)^{a} \left(Re_c \frac{\mu_c}{\mu_m}\right)^{b} \qquad (6)$$

where x is the distance from the slot

m is the mass ratio $\rho_c u_c / \rho_m u_m$

s is the slot effective thickness, equal to $\frac{\text{total area of injection orifices}}{\text{total span}}$

Re_c is the slot Reynolds number $\frac{\rho_c u_c s}{\mu_c}$

Typical values of constants for tangential slot cooling in incompressible flow are $k = 3.09$, $a = -0.8$, $b = 0.2$.

Another way of assessing the effective (or adiabatic) film temperature is to run an experiment with no convection cooling to steady state conditions and then to measure the wall surface temperature.

2.4. The behaviour of h_f along a film cooled surface

If equation (4) is used, then it is implied that the surface flow after injection has the characteristics of a boundary layer. Just downstream of injection through, for example, inclined holes, the flow is so complicated with three-dimensional effects and interactions with the outside flow that the normal boundary layer assumptions can no longer be considered applicable. This is demonstrated by the fact that under practical conditions the mass of coolant injected is often greater than the mass of fluid in the oncoming boundary layer itself.

In illustrating the effect of injection on the heat transfer coefficient, consider the case of the secondary fluid injected at such a temperature that its recovery temperature is the same as

the mainstream flow recevory temperature T_{rm}. Under this situation one can ignore the effect of the cooler gas on the heat transfer rate since equation (4) will become :

$$q_f = h_f \ (T_{rm} - T_{\omega o}) \qquad (7)$$

Now, injection through inclined holes has the effect of mixing the flow in the oncoming boundary layer and even the surrounding free stream fluid in a similar fashion to large roughness elements. It is well documented that during regions of roughness and downstream of it surface heat transfer rates are increased in laminar and turbulent flows (and also boundary layer transition is advanced if the flow is still laminar), hence if T_ω is kept the same, then from Eq.(7), h_f will be increased above its undisturbed value just downstream of roughness and hence fluid injection. However, roughness (and fluid injection) will have the effect of thickening the boundary layer and, at a distance far enough downstream from the disturbance that profiles revert to those similar to their undisturbed form, then q and hence h_f for the same wall temperature will be lower than its undisturbed value. This behaviour is in fact illustrated in some experiments by Choe et al (Ref.6 and demonstrated in a schematic in Fig.2) who have measured heat transfer rates in the region of and downstream of a full-coverage film cooled surface with the secondary fluid at the same temperature as the mainstream fluid in an incompressible flow situation.

At present there exists limited information concerning the behaviour of h_f with film cooling flow and geometry variables. Its importance in a design calculation is discussed in the next section.

2.5. Design application of adiabatic wall effectiveness information

Introducing the definition of the effectiveness given by Eq.(5) in the expression for the heat transfer rate to a film-cooled surface (Eq.4), we obtain :

$$q_f = h_f (T_{rm} - T_{\omega o})(1 - \eta\theta) \tag{8}$$

on further introducing Eq.1 :

$$\frac{q_f}{q_o} = \frac{h_f}{h_o} (1 - \eta\theta) \tag{9}$$

where θ is a compressible flow version of the non-dimensional temperature parameter first introduced by Metzger et al (Ref.7) defining the level of the coolant temperature with respect to the wall temperature in terms of the mainstream temperature.

$$\text{i.e. } \theta = \frac{T_{rm} - T_{rc}}{T_{rm} - T_{\omega o}} \tag{10}$$

In a design case, to calculate the heat transfer rate to a film cooled surface, then it is seen that one requires both h_f and η as well as the flow temperatures T_{rm} (which for subsonic flows can be safely assumed to be equal to the flow total temperature), $T_{\omega o}$ and T_{rc}. As explained in section 2.1., equation 8 will be applied iteratively with Eqs. 2 and 3 to arrive at the blade outer wall temperature, $T_{\omega o}$.

2.6. Isothermal wall effectiveness

The concept of adiabatic wall effectiveness applied in the last few sections originated from the earliest method of measuring film cooling effectiveness. This method involved measurement of the adiabatic wall temperature distribution downstream of fluid injection in steady state experiments. Early applications, such as aerodynamic surface de-icing and cooling, nozzle cooling, etc., required only information about the surface temperature under adiabatic wall (or zero surface heat transfer conditions) and the problem about the value of the heat transfer coefficient, hence, did not arise.

In application to turbine flows, film cooling provides a supplementary method of cooling above blade internal convection and impingement techniques. This means that the blade surface is no longer adiabatic and large heat transfer rates to the surface will exist, making the adiabatic wall concept unrepresentative. Early predictions of the heat transfer rate to film cooled surfaces however used the adiabatic wall effectiveness information then available applied to Eq.4 and assumed that h_f was equal to h_o, the undisturbed heat transfer rate coefficient. More recent research, e.g., Metzger (Ref.7) and Liess (Ref.2) has shown this not to be true as also was argued in Section 2.4.

For advanced turbines, the combined application of film cooling and convection cooling is being used in order to keep the blade at as constant a temperature as possible. There have resulted experimental programmes on film cooling in which the wall temperature is kept constant and heat transfer measurements taken (e.g., Metzger et al, Refs.7,8 ; Liess, Ref.2 ; and more recently Choe et al, Ref.6, and Crawford et al, Ref.9). Short duration wind tunnels, previously developed to solve high speed aircraft and re-entry space vehicle kinetic heating problems, have recently been applied to turbine comp-

onent cooling studies. In these facilities, in the normal mode of operation, the wall temperature is also kept constant (at laboratory levels). For these reasons, another means of defining effectiveness which may at first seem logical, is through the ratio of the heat transfer rates with and without film cooling.

A heat transfer coefficient has been defined (Louis et al, Ref.4) in terms of the temperature difference between the mainstream recovery temperature and the wall temperature as follows :

$$q_f = h\ (T_{rm} - T_{\omega o}) \tag{11}$$

Then the effectiveness can be gauged by the ratio of these newly defined heat transfer coefficients with and without injection (using Eq.1) as follows :

$$\frac{h}{h_o} = \frac{q_f}{q_o} \tag{12}$$

Following these lines, the so called isothermal wall effectiveness parameter has been introduced (Louis et al, Ref.4) defined as :

$$\eta_q = 1 - \frac{q_f}{q_o} = 1 - \frac{h}{h_o} \tag{13}$$

This has been shown to have similar characteristics as the adiabatic wall effectiveness by Schultz (Ref.10) inasmuch that for zero injection $q_f = q_o$ and hence $\eta_q = 0$. However only for the case of coolant temperature equal to the wall temperature for a perfectly applied film does one achieve the condition $q_f=0$ to give $\eta_q=1$. Note that in the situation when the coolant is less than the wall temperature, as is found in a practical situation in a turbine then q_f for a perfectly applied film will be negative

and η_q can be greater than 1. This cannot be the case for the adiabatic wall effectiveness.

The relationship η_q to η is found immediately from Eqs. 9 and 13.

$$\eta_q = 1 - \frac{h_f}{h_o}(1-\eta\theta) \tag{14}$$

It is interesting to note that if $h_f = h_o$ (i.e. the injection effectively causes no disturbance to the flow) and $T_{rc} = T_{\omega o}$ (i.e. $\theta = 1$) then the isothermal wall effectiveness is the same as the adiabatic wall effectiveness.

$$\text{i.e. } \eta_q = \eta \text{ for } h_f = h_o \text{ and } T_{rc} = T_{\omega o} \tag{15}$$

$$\text{also } \eta_q = \eta\theta \text{ for } h_f = h_o \text{ and } T_{rc} \neq T_{\omega o} \tag{16}$$

$$\text{and } \eta_q = 1 - \frac{h_f}{h_o}(1 - \eta) \text{ for } T_{rc} = T_{\omega o} \text{ and } h_f \neq h_o \tag{17}$$

The value of q_o in experiments may be obtained by carrying out tests in which there was no coolant injection. Care must be taken here in that due to wall perturbations caused by the injection holes the heat transfer rate may be different than if the wall was impermeable as found by Lander, Fish & Suo (Ref.11). In the design case q_o may be calculated by appropriate boundary layer solution as outlined by Richards (Ref.12).

2.7. The design application of isothermal wall information

It is noted that in the definition of h given by Eq.11, the only parameter within that can reflect the coolant temperature effect is h. Its effect can be seen in relation to the non-dimensional cooling parameter by combining Eqs. 8 and 11, i.e.

$$h = h_f (1 - n\theta) \tag{18}$$

which equation is plotted in Fig.3 with the heat transfer coefficients non-dimensionalised by dividing by h_o. This relationship was originally developed by Metzger et al (Ref.7) who demonstrated the linearity by experiments carried out at different values of θ, created by changing $T_{\omega o}$. Later Metzger et al (Ref.8) defined the curve from measurements of h at different wall temperatures and then used the resulting relationship to extrapolate the curve to $\theta = 0$ to obtain h_f and to $h = 0$ to obtain $n = 1/\theta_{h=0}$ thus providing a different method to obtain adiabatic wall effectiveness and heat transfer coefficient, h_f, than directly measuring the adiabatic wall temperature and measuring the heat transfer rate at another wall temperature as used by Liess (Ref.2) for example. For a similar application to full-coverage film cooling Choe et al (Ref.6) and Crawford et al (Ref.9) demonstrated on the other hand the linearity in h and θ implied in Eq.18 by changing the coolant temperature at approximately similar wall temperatures rather than change wall temperature at constant coolant temperature as did Metzger. As yet it has not been demonstrated experimentally that the variations of h with θ using firstly a change in the wall temperature and secondly a change in coolant temperature will coincide, but the "superposition" analysis by Choe et al (Ref.7) provides reasonable confidence that this will be true for incompressible flow and small temperature differences.

These latter authors chose to display the film cooling data by providing h at $\theta = 0$ and $\theta = 1$ (obtained by changing T_{rc} from T_{rm} to $T_{\omega o}$) giving a designer an opportunity to obtain h at any value of θ using the relationship :

$$h = h_{\theta=o} - \theta(h_{\theta=o} - h_{\theta=1}) \qquad (19)$$

This method was chosen for its appropriateness to full coverage film cooling (which has similarities with transpiration cooling in which h is always used as the heat transfer coefficient), however for surfaces downstream of injection the same information could be used to obtain $h_f (= h_{\theta=o})$ and η (from $\eta = 1/\theta_{h=o}$) by appropriate extrapolation (see Fig.3) and then to use Eq.18 instead of 19 as done by Metzger (Ref.8).

From this discussion arising from linearity of the temperature field implied by Eqs. 4 & 11, it is seen that the film effectiveness cannot be defined just by the single parameter η_q in the same way as η, but it must be supplemented by an indication of the value of θ at which it is obtained. Following the arguments of Choe et al (Ref.6), considerably more flexibility can then be given to the designer by giving him η_q (or q_f or h) at another value of θ enabling him to obtain q_f at the various values of $T_{\omega o}$ and T_{rc} encountered during his design iteration. It should be remarked also that the value of η as obtained from adiabatic wall measurements may differ from that obtained by applying the above mentioned isothermal-wall-approach, since the upstream flow field development will be different in each case (Choe et al, Ref.6).

The assumption about linearity of the temperature field should be questioned at this stage for the design case in which the total,wall and coolant temperatures are at levels of the order of 2000 K, 1200 K and 600 K respectively for a future projected turbine.

The fluid temperature and hence the gas density gradients are so high as to suspect the inacurracy of an assumption concerning a constant property fluid even though the flow Mach number may be small. The conditions are also far removed from the incompressible small temperature variation flows under which the linearity of Eq.8 was proved experimentally in Refs.6 and 7. For example, the same value of $\theta = 1.75$ can be obtained for the design case indicated above in which $T_{rc}/T_{rm} = 0.3$ and $T_{\omega o}/T_{rm} = 0.6$ as can be obtained in a typical incompressible or compressible "film heating" experiment in which $T_{rc}/T_{rm} = 1.117$ and $T_{\omega o} = 1.967$. This demonstrates that apart from θ, another temperature parameter should be used to define the conditions of the test, e.g. $T_{\omega o}/T_{rm}$.

Another reason for suspecting non-linearity in the temperature field may be demonstrated from the fact that if in the design case mentioned earlier θ is changed from 1.75 to 1 (i.e. a change in coolant temperature from 600 K to 1200 K), then for a representative but the same value of m, the coolant flow velocity will be typically increased by 58% and its density will be decreased by 37%. These changes in conditions are enough to seriously change the mixing characteristics of the film with the outside stream which may cause non-linearities. Furthermore, film "lift off" is likely to occur at a different m depending on the coolant temperature.

No experimental evidence is as yet available, for the design case of compressible flow with large temperature differences, to verify that linearity in the temperature field (hence in eqs.4 and 11) is indeed achieved. Until an appropriate study is made, it is recommended that measurements of film cooling effectiveness for design purposes be carried out at as close to simulated conditions as possible to keep errors in extrapolation as small as possible.

2.8. Development of empirical prediction techniques

The number of variables that influence film cooling effectiveness is very large. The approach leading to accurate prediction of the phenomena involved would be expected to involve initially comparative studies to select the most likely coolant orifice geometries in terms of effectiveness and practicality. This need not involve testing at this stage under fully simulated flow conditions. The geometrical variables may include orifice shape (circular, rectangle, etc) and size, angle of inclination in a streamwise and crosswise sense, spanwise and streamwise orifice spacing, number of rows, stagger angle, distortions of orifice near surface, etc... An idea of the degree of effectiveness achievable for the case of a perfect applied film may be assessed by comparison with ideal analyses such as that given in Section 2.3.

In this latter analysis, it may be noted that all mainstream flow variables are lumped into an expression for the mass flux variation of a boundary layer as a function of distance and so no explanation of such effects as M, Re, curvature, pressure gradient, turbulence, etc, appears. Furthermore, the contribution of the coolant is lumped into the two parameters $m = (\rho_c u_c / \rho_\infty u_\infty)$ the mass flux ratio, and the effective slot height s. In this case, no information about the orifice geometry is included. Nevertheless the method describes the physical behaviour fairly well and can be used as the basis for empirical correlations. Comparative studies of the degree of deviation of experiment from this simple analysis for changes in flow and geometrical variables not included in this theory are also necessary at conditions which need not involve testing under simulated conditions. Final calibration of empirical theories arising from such test programmes should however be finally carried out at conditions closely simulating actual operating conditions, i.e., full simulation of M, Re, $T_{\omega o}/T_{rm}$ and T_{rc}/T_{rm} (or θ).

2.9. Concluding remarks

Film cooling of gas turbine components is applied practically under approximately isothermal wall heat transfer conditions, rather than under adiabatic wall conditions. It is hence considered more appropriate to provide test data at such isothermal wall conditions rather than attempt to measure directly the adiabatic wall temperature, even though this latter parameter given as the film effectiveness parameter, η, provides a useful piece of information and hence should be available. With a further assessment of the film heat transfer coefficient, $h_f = q_f/(T_{a\omega}-T_\omega)$ for a particular value of x, $m = \rho_c u_c/\rho_m u_m$ and external flow condition, then it has been inferred from analysis and experiment that the heat transfer rate at any value of T_{ω_o} and T_{rc} can be assessed through the equation :

$$q_f = h_f\,(T_{rm} - T_{\omega o})\,(1 - \eta\,\theta) \qquad (20)$$

for incompressible flow and small temperature differences.

The values of h_f and η can be obtained by measuring q_f at two different values of θ achieved by <u>either</u> changing the wall temperature <u>or</u> changing the coolant temperature under isothermal wall conditions and carrying out appropriate extrapolations. For direct application of this method to turbine flows, the linearity and uniqueness of Eq. 20 must be verified under more truly representative conditions of compressible flow, large temperature differences and representative injection configurations. Furthermore, in generating practical information of η and h_f, accuracy is expected only if all of the parameters M, Re, T_ω/T_{rm} and T_{rc}/T_{rm} (or θ) are simulated. The means of achieving this using short duration wind tunnels is explained in the following chapter.

3. EXPERIMENTAL EQUIPMENT

3.1. Justification of using short duration wind tunnels

The importance of carrying out experiments on film cooling of turbine components at well simulated conditions has been demonstrated in the last chapter. However, the power levels required to achieve such conditions of high temperature at representative pressure levels in a test rig are very large. A continuous facility running at high power is expensive to construct and operate. The main objective of short duration wind tunnels is to reduce the total energy invested in heating the working fluid by orders of magnitude whilst keeping the power level high. The temperature level of the tests is also changed such that the component under examination is at room temperature. Both it and the facility undergo such small changes in temperatureduring the running time that conventional materials and accurate heat transfer instrumentation can be used. Furthermore the conventional testing arrangement is that the model is isothermal, a condition that the designer is striving to achieve in choosing his cooling systems. In summary, the advantages of these facilities are good flow simulation at low cost and low power requirements with accurate measurement of heat transfer rates.

Following the analysis in chapter 2 and by Louis (Ref.13), it is evident that the temperature levels be scaled down by a factor of proportionality of operational wall temperature, T_{op} to ambient temperature ($T_{\omega o}$) given by :

$$S = \frac{T_{\omega o}}{T_{op}} \qquad (21)$$

The same scaling S should also be applied to the mainstream and secondary gases ; the mainstream gas heated by shock or isentropic compression for example, and the secondary fluid cooled by means of a

liquid nitrogen heat exchanger (e.g., Louis et al, Ref.4) to appropriate levels.

The modelling requirement that the Reynolds number and Mach numbers remain unchanged leads to an identical Nusselt number for operating and simulated flow conditions when it is assumed that the Prandtl number is unchanged. It can also be shown that the pressure level from operating (P_{op}) to experimental (P_{ex}) conditions is of the form :

$$\frac{P_{ex}}{P_{op}} = S \qquad (22)$$

when the characteristic lengths, ratio of specific heats, molecular weights are unchanged and a viscosity proportional to the square root of temperature is assumed.

To give an example for the first stage of a hypothetical advanced turbine, operating at high load, with a maximum blade temperature of 1200°K, a turbine entry temperature of 2000°K and a coolant temperature of 600°K, and a stagnation pressure of 20 bars, the equivalent simulated testing conditions will be $T_{\omega o}$=300°K, T_{rm}=500°K, T_{rc}=150°K and P_o=5 bars.

Shock tunnels operating in the reflected mode have been adapted to the subsonic, transonic and low supersonic flows desired in turbine studies (Refs.3,4). Jones et al (Ref.14) of Oxford University recognized that since a maximum experimental T_{rm} of 600°K is needed, an appropriate testing medium could be achieved easily using a pure isentropic compression cycle and a new heat transfer facility concept, the isentropic light piston tunnel (ILPT), was devised. The principle of operation is described in the next section. The advantages of the ILPT over a shock tunnel are that it is more compact, mainstream flow

conditions can be changed very flexibly and diaphragms need not be used to initiate operation such that more runs can be accomplished in a short period (Richards, Ref.15). Such short duration facilities have proven their usefulness both for heat transfer studies and for turbine aerodynamic studies at Oxford University. The ILPT approach has been adopted by VKI in its continuing research into turbine film cooling and has constructed a small version whose test section is being used to simulate the flow between two adjoining turbine blades (see next section). A larger hot cascade version, with a test section size the same as an existing VKI cold cascade tunnel, is under construction and will be used in later stages of the present research programme. The former facility develops 60 kw power in a test section size of 13 mm × 16 mm, and the latter up to 1 MW power in a test section size of 300 mm × 100 mm both over periods of about 1/10th second.

3.2. Description of isentropic light piston cycle

The principle of the facility is illustrated in Fig.4. The test gas is contained in a tube and is compressed and heated isentropically by a piston which is propelled by gas entering the tube from a high pressure reservoir. When the test gas has been compressed, and hence heated to the required temperature, it is allowed to flow through the test section and the pressure within the tube may be maintained constant if the volumetric flow rate of gas into the tube from the high pressure reservoir is the same as that leaving through the test section. The facility is then operating in what is known as the "matched" mode. The starting of the test flow is normally by the breaking of a diaphragm or the quick opening of a shutter valve.

The result of the cycle, in theory, is initially to create a monotonically rising pressure in the tube, which then remains

constant between the time that the test flow starts and the piston reaches the end of the tube. After this latter event the pressure in the tube then continues to rise until the reservoir gas flow is stopped. The pressure, and hence temperature, variation seen in the test section is then expected to follow a step-like variation as illustrated in Fig.4. Such a behaviour of flow is most suitable for the application of transient techniques for measuring heat transfer rates on surfaces, but at the same time has a long enough running time that a wide range of not necessarily highly sophisticated pressure transducers can be used.

The theory of the concept has been thoroughly dealt with in Jones et al (Ref.14) and in the preceding paragraphs only the main features are presented.

3.3. VKI Tunnel CT-1

The Institute's isentropic light piston tunnel, CT-1, shown in Fig.5, was fabricated from a disused shock tube. The tube, having a well polished interior bore of 102 mm is 3.25 m long (volume 0.0266 m^3). This was connected by a 25 mm tube to an existing high volume air reservoir delivering up to 40 bar to the tube, through an orifice of 0.675 cm^2. The various test sections each having throat areas of approximately 1.5 cm (one with a diameter of 14 mm, the other with a 15.7 × 13.4 mm section) connecting the tube to the dump tank (this latter consisted of the original shock tube driver section of 1.25 m length supplemented by another reservoir giving a volume of equivalent size to the tube). The whole system was hydraulically tested for operation up to 40 atmospheres. Normal operation, however, involves using the facility only up to 20 atmospheres. A nylon piston fitted with 2 nylon piston rings (to reduce leaks to a minimum in the slightly uneven bore, while retaining its necessarily smooth running capability)

weighing only 60 gm, of approximately 5 cm length and having good rigidity is used. Readily available PVC tape (scotch tape, selotape, tesa tape are suitable) of differing thickness (0.065 and 0.1 mm) is applied to the flat surfaced entry to the nozzles to act as diaphragms. Such diaphragms give reasonably repeatable breaking pressures, which depend on the temperature of the gas aimed for.

Up to present, subsonic operation has been achieved by using a constant area test section with a downstream throat. Because of this and the normally high pressure conditions used, it has been possible to operate with the dump tank at atmospheric pressure. For lower pressure conditions the dump tank is evacuated. Before firing the tube is charged with the desired initial pressure (either slightly pressurised or slightly evacuated). After presetting the instrumentation the tunnel is set into operation by opening quickly a manually operated ball valve. After the test, the system is brought to room pressure, the test section uncoupled from the tube and the diaphragm replaced ready for the next test. The turn round time for operation can be less than five minutes.

3.4. Instrumentation

The tube pressure (and sometimes test section static pressures) is measured with a Validyne type DP15TL variable reluctance diaphragm transducer. Static pressures are measured using either Hidyne type W variable reluctance transducers (for pressure levels less than 2 atmospheres, as obtained in supersonic flow tests) or Kistler or PCB quartz piezoelectric transducers (for higher pressures). Heat transfer rates are measured using standard thin film platinum resistance thermometers painted on pyrex or quartz inserts in the model. These thermometers are used in conjunction with appropriately designed analogue units. (See Schultz and Jones, Ref.16, for details of this instrumentation).

In film cooling experiments, mass flow rates are measured by monitoring the pressure variation in a 1,500 cm^3 reservoir with a 7 atm pressure limitation during the tests. This method appeared to be the only one available with sufficiently fast response time to measure the flow rate during the test itself, of importance when dealing with an unchoked feed system. For studies of film cooling of a developmental nature, two similar coolant feed systems have been built, but with a pressure capability of only 3atm. These were not used in this study.

Flow temperatures are measured using fine tungsten wires (5-10 μm) as equilibrium temperature probes. The temperature is assessed from the change in resistivity of the wire during the test, and this value is corrected for conduction end losses to the wire supports, and radiation losses (Backx, Ref.17). Response times of less than 1 μsec are achieved, and because of this the technique has a great advantage over others in that any subtle disturbances away from that expected can be easily detected.

Except in some cases, UV oscillographs with speeds up to 256 cm/sec are used for recording the signals from the instrumentation. Galvanometers with response times up to 5 kHz are available, and sufficient for most purposes. Oscillographs have advantages over oscilloscopes in terms of cheapness per test (expensive polaroid film has normally to be used to record oscilloscope signals) and little difficulty in its triggering. Galvanometer drive units have been fabricated by the Institute to vary easily the recording system sensitivity and facilitate system calibration.

To synchronise the various events during operation with coolant injection, a trigger and delay system has been designed and built. A triggering pulse is set-off from the achievement of a "threshold voltage" by the processed signal from the Validyne transducer monitoring the tube pressure. This pulse is used to

trigger the single trace on the oscilloscopes and to activate the solenoid valves which initiate injection. The oscillographs are started manually at the same time as the reservoir valve is opened, and stopped automatically after a suitable time lag to encompass the tunnel running time.

3.5. Models

The film cooled test surface is one wall of the 13.4 mm × 15.7 mm rectangular test channel of CT1. Typically, downstream and on the centre line of the plate of an injection section, 15-20 thin film platinum resistance gauges (with dimensions of 3 mm span by 0.5 mm chord) are positioned within a length of 50-70 mm. These gauges average the spanwise heat transfer rate distribution across a number of injection holes. A two-dimensional streamwise slot facing upstream is installed on the test surface 41 mm upstream of the injection position to act as a flow bleed. The test channel can further be modified to alter the geometry to create either a pressure gradient on the test surface or to give it curvature.

The geometry of the coolant injection system selected was as follows :

hole diameter, d	:	0.5 mm
spanwise spacing	:	1.0 mm
number of rows	:	2
injection angle	:	30°
spacing between rows	:	1.5 mm on surface
injection channel length	:	8 mm
number of holes	:	25

The base selected for study was :

$$\left.\begin{aligned} M_m &= 0.6 \\ p_{0m} &= 8\text{-}9 \text{ bars} \\ T_{0m} &= 510\text{-}522 \text{ K} \end{aligned}\right\} \quad Re_m = 4 \times 10^7/m$$

$$T_{oc} = 293 \text{ K}$$

$$T_{\omega o} = 293 \text{ K}$$

Scale drawings of the test models used in the present study are given in Fig.6. Model A has a flat test surface with a constant area test section with a constant area section providing a zero pressure gradient. Models B and C have convex curved test surfaces with radii of curvature of 130 mm and 65 mm respectively and with constant area sections. The curvatures were chosen to have similar curvature as representative turbine blades. Model D is similar to model A but with the opposite wall to the test surface contoured in such a fashion as to provide a constant favourable pressure gradient of 170 mmHg per cm at p_{om}=8.4 bar starting at the injection position. This pressure gradient is typical of that achieved on a typical turbine blade. The boundary layer bleed had a height of 4 mm for models A,B and C and 5 mm for model D.

4. EXAMINATION OF A METHOD OF MEASUREMENT OF ADIABATIC WALL TEMPERATURE USING A TRANSIENT TECHNIQUE

4.1. Introduction

In the short duration facilities such as the VKI Isentropic Light Piston Tunnel CT1, heat transfer is measured using the thin film platinum resistance technique. It is obtained from temperature measurements of the surface of a "semi-infinite" slab of pyrex glass either numerically by the use of an electrical analogue circuit, or by the following solution of the appropriate one-dimensional heat conduction equation :

$$q(t) = \frac{\sqrt{\rho c k}}{2\sqrt{\pi}} \left\{ \frac{2T_\omega(t)}{\sqrt{t}} + \int_0^t \frac{T_\omega(t)-T_\omega(\tau)}{(t-\tau)^{3/2}} dt \right\} \qquad (23)$$

where ρ, c, k, are the density, specific heat and conductivity of the pyrex backing material, t is the time and τ is a dummy variable of time.

The technique is applied so that near the beginning of a test the test surface is isothermal.

Because of the length of running time and size of heat transfer rates generated by this facility, the adiabatic wall temperature is never achieved during a test, but sufficient time elapses such that the heat transfer rate is sampled at a range of wall temperatures. If we can make a statement about the behaviour of h_f and $T_{a\omega}$ during a test (e.g., that they remain constant during a test) then sufficient information to evaluate these parameters is available from the measurement of wall temperature and heat transfer rate during a test and the use of equation (4). The evaluation will be more accurate the closer that T_ω approaches $T_{a\omega}$. One further test in which no cooling is

applied can be used to verify the already well-defined (from knowledge of the test conditions) values of T_{rm} to be able to obtain η in equation (5).

An experimental study was carried out to determine the possibility of determining the adiabatic wall temperature from the wall temperature changes and heat transfer rate data obtained during tests in CT1. An initial indication of the success of such a method should be obtained by attempting to determine the adiabatic wall temperature without injection, a value which can be assessed accurately from measurements of the flow temperature.

4.2. Tunnel characteristics

In testing out such a technique in CT1, the main difficulty encountered was that small fluctuation in pressure during a test caused by the use of a finite weight piston, is sufficient to create fluctuations of flow temperature, related to $T_{a\omega}$ of the same order as the wall temperature variation. The resulting behaviour of the difference in temperatures, $T_{a\omega}-T_{\omega}$, and the implied variations in h create uncertainties.

During a test in CT1, measurements of pressure at nominal conditions of 7.0 atm., and 540 K show that the fluctuations, with the shape of sine waves, occur with typically a peak-to-peak amplitude of 3.7 % of the supply pressure and a period of about 23 msec giving the following relation :

$$p = p_o - \Delta p \sin Kt = p_o\left(1-\frac{\Delta p}{p_o}\sin Kt\right) \qquad (24)$$

where $K=2\pi/T$ and T is the period of the oscillation (see Fig.5).

Since the flow behaviour in the central core region of the compression tube (i.e., away from wall boundary layers) is isentropic, the temperature variation is expected to be quite

similar but to a power of 2/7. Careful measurements of temperature with a fine wire probe, developed at the Institute by Backx (Ref.17), show that fluctuations in temperature occur with the expected amplitude, but also that the temperature increases from a slightly lower value than expected from an isentropic compression of the gas to achieve the expected value at about 40 msecs from the start of the test. This behaviour is ascribed to the formation of a ring vortex just upstream of the diaphragm containing colder test gas than in the core. This colder gas mixes with the core gas during the early part of the test. It is pointed out that this effect, small even in this prototype tunnel, will not be noticably evident in the 1 meter diameter CT2 tunnel being installed in the Institute, because of the smaller relative size of the wall boundary layer in the latter case. The temperature variation with time hence may be approximated by the following equation :

$$T = T_o \left\{ 1 - (1-t/40) \frac{\Delta T_1}{T_o} - \frac{\Delta T_2}{T_o} \sin Kt \right\} \qquad (25)$$

In the present facility at nominal test conditions of $P_o = 7$ kg/cm^2 and $T_o = 540$ K, $\Delta T_1/T_0 \simeq 0.02$ and $\Delta T_2/T_0 = 0.0053$.

To illustrate the sensitivity of such fluctuations in flow supply pressure (causing fluctuations in supply temperature due to the isentropic relationship) on various flow parameters, calculations were made and are here presented briefly : a 10 % increase in supply pressure, with a 2.76 % increase in supply temperature causes a 1.9 % increase in flow viscosity, a 1.4 % increase in flow velocity, a 1.8 % increase in reference temperature, and 8.1 % increase in density, a 1.4 % increase in viscosity based on reference temperature conditions, and 8.1 % change in Reynolds number (based on reference conditions), a 1.3% decrease in skin friction at 10 cm from the origin of a turbulent boundary layer, and finally an 8.1 % increase in heat transfer coefficient h and a 15.6 % increase in heat transfer rate q.

It can be seen that, considering that the pressure fluctuations measured are usually less than 4 % peak-to-peak, resulting fluctuations in T_{om} (which is nearly equal to T_o at the M = 0.5 conditions considered) and h are small, but not negligible. These calculations were made assuming an Eckert reference temperature method for determining c_f and hence q.

4.3. Method of calculation

In order to account for the flow variation described earlier, Eq. 4 was modified to :

$$q(t) = h_{ref}\ (1+\beta(t))\ \{(T_{a\omega})_{ref}\ (1+\alpha(t))-T_{\omega}(t)\} \qquad (26)$$

where q(t) and T(t) are the measured values from the tests, h_{ref} and $(T_{a\omega})_{ref}$ are reference values of h and $T_{a\omega}$ to be calculated, $\beta(t)$ is given by :

$$\beta(t) = -\frac{\Delta h}{h_0} \sin Kt \qquad (27)$$

where K is as defined in Eq.24 and $\Delta h/h_0$ is assumed to be 0.81 $\Delta p/p_0$ from the observation given in the last paragraph ; $\alpha(t)$ is given by (on reference to Eq.25) :

$$\alpha(t) = -(1-t/40)\ \frac{\Delta T_1}{T_0} - \frac{\Delta T_2}{T_0} \sin Kt \qquad (28)$$

In using Eq.(26), h_{ref} and $(T_{a\omega})_{ref}$ should be non-varying during a test. The method used to solve this is to guess a value for h_{ref}, then for about 10 measurements of T_w and q taken at equal time intervals during the part of the run when these parameters are changing the most, $(T_{a\omega})_{ref}$ is calculated. Another value of h_{ref} is selected for the next iteration. If $(T_{a\omega})_{ref}$ has a decreasing trend with time, a

larger value of h_{ref} should be selected, and vice-versa. Such iterations are continued until it is assessed that $(T_{a\omega})_{ref}$ is invariant. The resultant values of h_{ref} and $(T_{a\omega})_{ref}$ are taken as solutions of the equation.

4.4. Results of tests carried out to determine adiabatic wall temperature without injection

The calculation method described was computerised in order to obtain a higher accuracy in the iteration scheme. As an input to this method, the following experimentally determined properties were used :

- Total and static pressure (P_{om}, P_s), resulting in detailed information on the pressure fluctuations,
- Wall temperature (T_ω),
- Heat transfer rate (q), determined experimentally and by numerical integration of T_ω

The fluctuations on the values of h_f and $T_{a\omega}$ are related, as explained before, to the pressure fluctuations, using sine wave approximations but also, however, the experimentally determined fluctuations. The scatter on $T_{a\omega}$, calculated this way, was approximately 15 %, but with all values being below the expected result.

This observation coupled with a slight but continuous drop in temperature measured at some time after a test has started gave an indication that viscous effects occurring in the tube during the compression and/or testing periods even larger than originally expected are causing gradients of temperature across the test section. The simplest way to test out this possibility was to bleed off a considerable part of the flow near the wall and remeasure $T_w(t)$ and $q(t)$. Such tests carried out using a 5 mm high bleed did indeed provide a better alignment of $T_{a\omega}$ with T_{0m}, although as expected from the method

used in which a gross extrapolation is used approximately the same 15 % scatter was obtained.

From these experiments it is tentatively concluded that a temperature gradient, caused by viscous effects in the compression tube, is present which caused a cool layer (presumably thicker than the growing boundary layer) to exist near the wall. In all future tests a bleed is used.

It is pointed out that in the larger tunnel CT2, because the pressure and temperature levels will be similar to CT1, the relative size of such viscous effects will be considerably smaller. Furthermore, the test models used will be situated in the main core of the free stream, which will be expected to be unaffected by viscous effects.

4.5. Discussion of possible methods for determining adiabatic wall effectiveness with injection

The method outlined in the last section can be applied to the method of determining adiabatic wall effectiveness with injection. The accuracy would be expected to be similar because of the nearly proportional relationship between q and the difference $(T_{a\omega}-T_{\omega})$. The accuracy of this method has not been verified since values of the film adiabatic temperature are not known accurately a priori in the same way as is the mainstream recovery temperature.

For zero injection as well as with injection, another method of determining n and h_f (or h_o) is to change the initial wall temperature by pre-heating or cooling the model and extrapolating the heat transfer rate variation with wall temperature approximately (see Section 2.7.). The disadvantage of this method is that it would severely complicate the test set up, a trend away from the simplicity of the normally ambient

temperature operating thin film heat sensors. Nevertheless, at a research rather than developmental level, it would be interesting to carry out a test series to determine the linearity of Eq.20.

A third possibility would be to inject coolant at different temperatures, assume that Eq.20 is linear and unique for a particular injection geometry, injection rate, position and flow condition, and extrapolate the trend in h with θ in the fashion described in the last section.

4.6. Concluding remarks

An investigation was carried out into the possibility of measuring the adiabatic wall temperature from time dependent measurements of heat transfer rate and wall temperature made using the thin film transient technique in the CT1 short duration tunnel. The results indicated that the method examined produced large uncertainties on account of the requirement for a large extrapolation of data obtained during slightly non-steady test conditions. Development of this method will be dropped until the new tunnel CT2 is in operation.

Two other possible methods are outlined, one by changing the initial wall temperature or the other by changing the coolant temperature respectively in successive tests. The accuracy of these methods will be examined in future test programs.

5. EXPERIMENTAL STUDY OF THE EFFECT OF CHANGING FLOW PARAMETERS ON FILM EFFECTIVENESS

5.1. Introductory Remarks

The intention of this part of the study was to examine the effect of Mach number, Reynolds number, wall curvature and pressure gradient on film cooling effectiveness. Each of these parameter changes occur due to the flow over a turbine blade and representative values are selected in these tests. Since this is a comparative study then it is not considered essential that the adiabatic film cooling effectiveness η and the heat transfer coefficient h_f be assessed. It will be sufficient to take the ratio of heat transfer rates at isothermal wall conditions and $T_{rc}=T_w$ as given by Eq.12 as the parameter to gauge the effectiveness.

One should be reminded of the result of the simple prediction method given in Section 2.3 which does not incorporate all of these variables under examination in its formulation but yet is widely used for predicting film effectiveness under widely diverse conditions. The degree to which one can apply such theories under realistically simulated conditions of $M, Re, T_w/T_{rm}$ (but not exactly T_{rc}/T_w) can thus be assessed.

5.2. Heat transfer on a surface without coolant injection

Measurements of the heat transfer rate from model A at the base conditions of P_o= 9 bars, T_o=522 K, M=0.6, Re=4.8×10^7/m T_{wo}=320 K (measurements were taken 10-15 msecs after the start of the test) without coolant injection are illustrated in Fig.7. In this case, the perforated injection piece was replaced by one without holes, thus ensuring a smooth surface. The measurements were compared with the semi-empirical theory of Spalding and Chi (Ref.18) which slightly over-predicted them. In applying the theory, the von Karman-Reynolds analogy factor was applied.

The heat transfer rates on the two curved surfaces are presented in Fig.8. It can be seen that the heat transfer rate diminishes with surface curvature. This trend agrees with the results of Thomann (Ref.19) for supersonic flow, which could be explained by changes in turbulence structure caused by streamline curvature (Bradshaw, Ref.20). Surface flow visualisation using oil illustrated an increasing trend of secondary flow behaviour with increasing curvature in this small channel which could also cause the observed trend of decrease in heat transfer distribution.

5.3. Results of film cooling study

The scope of the film cooling tests is given in Table 1. Presented are the external flow conditions (M, P_0, T_0, Re, dp/dx), the model geometry (R) and the injection rate parameter (m). In all cases the data was taken with the wall temperature and coolant temperature the same and equal to ambient laboratory conditions.

The relationship between m and the coolant pressure ratio p_{oc}/p_∞ for each of the 3 basic flow conditions are presented in Fig.9. The sensitivity of the coolant injection rate parameter to Mach number is illustrated here.

The basic results, given as q_f/q_o against x/d for all tests are presented in Figs.10-16. A measure of the film cooling effectiveness is given by $\eta_q = 1 - q_f/q_o$ (where $\eta_q = \eta$, when $T_{oc} = T_w$, and $h_f = h_o$ as illustrated in Section 2.6). The results show the general trends of decreasing effectiveness with downstream position, and increasing effectiveness with increasing coolant mass flow rates. There are a few exceptions to the latter trend at high values of m and low values of x/d, as in Fig.10, $m = 1.7$. This signals the onset of flow lift-off by the coolant. It is interesting to note that with these low (but well simulated) values of coolant to mainstream temperature

ratio, the level of m for lift-off is much higher than for cases in which the coolant is closer to or higher than the mainstream temperature (e.g., Liess, Ref.2). Further observation of the effects of other parameters on effectiveness are given later after appropriate correlation of the data outlined in the next paragraph.

Using the boundary layer model outlined in Section 2.3., then one would expect that the parameter $\bar{x} = \frac{x}{ms}.(Re_c \frac{\mu_c}{\mu_m})^{-1/4}$ would collapse the data from each test series.
An illustration of the applicability of this correlation is illustrated in Fig.17. It can be seen that the data in the range $0.5 < m < 1.7$ collapses well on a curve, which at high values of $\bar{x}$ is well represented by the equation $\eta_q = 1.5 \ (\bar{x})^{-0.8}$ This illustrates that at positions far from injection the boundary layer model gives the correct trend in behaviour. However, it is obvious that film cooling through discrete holes is considerably less effective than if the coolant was injected in a streamwise direction from a slot, by comparing this relation with the experimentally verified variation of $\eta = 3.09 \ (\bar{x})^{-0.8}$ for slot cooling (Stollery and El-Ehwany, Ref.5).

The same correlation procedure has been applied to the remaining data and presented in Figs.18-23. The resulting value of the constant in the equation $\eta = \text{const} \ (\bar{x})^{-0.8}$ provides a means of comparing the change in effectiveness due to change in flow parameters, as well as gauging the effectiveness of a coolant system with injection through inclined holes compared with a tangential slot system. It is interesting to note that the maximum effectiveness ever achieved by this coolant hole configuration is of the order of 0.8 for the lowest values of $\bar{x}$ (i.e., at high values of m at low x).

5.4. Discussion of results

5.4.1. Effect of surface curvature

At large values of $\bar{x}$, the data from the 130 mm radius plate (model B, Fig.18) follows a trend of $\eta_q = 1.67(\bar{x})^{-0.8}$ whilst the data from the 65 mm radius plate (model C, Fig.19) is considerably more scattered and follows an approximate trend of $\eta_q = 1.56(\bar{x})^{-0.8}$ The results indicate that there is a small increase in effectiveness due to convex curvature, although there is little apparent change by using a 65 mm rather than 130 mm radius. The scattered results occuring for the smaller radius curved surface, may be associated with the secondary flow effects observed. Under these circumstances, then the boundary layer model would be expected to break down, resulting in the choice of $\bar{x}$ as the correlative parameter being a poor one.

5.4.2. Effect of Reynolds number

The effect of Reynolds number can be examined by comparing the results from Fig.20 (in which the trend at high $\bar{x}$ is $\eta=1.2(\bar{x})^{-0.8}$) taken at M=0.6, $Re=4\times10^7$, $T_0=510K$ with those of Fig.21 (in which the trend is $\eta=1.3(\bar{x})^{-0.8}$) at M=0.6, $Re=2.35\times10^7/m$ and $T_{om}=425K$.

The Reynolds number change was accompanied by a mainstream temperature change as well which slightly obscures the result. However, it can be seen that the lowering of the Reynolds number (but with an accompanying decrease in mainstream temperature) causes a very small increase in effectiveness.

It is seen that at low values of m, in Figs.19 and 20 (as well as in 21), the effectiveness correlates poorly with $\bar{x}$. These tests were carried out at an earlier stage in the program than other tests when a less sophisticated mass flow measuring system was used for measuring these very low injection rates.

It is thus thought that the estimate of m is in error in this particular region. It is intended to examine this departure in more detail in future tests.

5.4.3. Effect of Mach number

The effect of Mach number can be examined by comparing the results of Fig.21 (in which the trend at high $\bar{x}$ is $\eta=1.3(\bar{x})^{-0.8}$) at M=0.6, Re=2.35×10^7/m and T_{om}=425K with those of Fig.22 (in which the trend is given by $\eta=0.93(\bar{x})^{-0.8}$) taken at M=0.3, Re=$2.35\times10^7$/m and T_{om}=510K. Again the Mach number change was accompanied by a mainstream temperature change. However, it can be seen that the lowering of the Mach number from 0.6 to 0.3 (but with an accompanying small increase in mainstream temperature) causes a sizable decrease in effectiveness.

5.4.4. Effect of pressure gradient

Finally, the effect of a favourable pressure gradient (typical of that seen on a turbine blade) on effectiveness can be examined by comparing the results of Fig.22 taken at M=0.3, Re=2.35×10^7/m, T_{om}=510K and zero pressure gradient with those from Fig.23 taken with the same conditions at injection but with an imposed favourable pressure gradient of 170mmHg/cm length along the length of the section until M=0.6 is reached. A dotted line through the results of Fig.22 is placed on Fig.23 for comparison purposes. It can be seen that the effectiveness is decreased by pressure gradient. It should be mentioned however, that the changing mainstream static temperature (which influences u_s) has not been included in calculating $\bar{x}$, but this variation is likely to have a very small value. The relatively significant Mach number trend described in Section 5.4.3. would tend to indicate an increase in effectiveness with downstream position an opposite trend to that seen. Hence, it must be concluded that this loss in effectiveness due to pressure gradient is a significant one.

6. CONCLUSIONS

An experimental study has been carried out to measure effectiveness of a film cooling system for a small turbine by injection through inclined holes. The flow conditions and model geometry were carefully selected to simulate those expected in an advanced turbine. Short duration testing techniques were used to provide data under isothermal wall conditions. The interpretation, usefulness and application to the design case of such data has been developed and the relationship between it and the conventional adiabatic wall temperature measurement approach is explained assuming a constant property flow field. A new line of research towards verifying the behaviour of film cooled boundary layers for the more practical case of variable property flows was suggested and preliminary work carried out in this direction. The final measurements showed that there are small increases in effectiveness for injection on convex surfaces compared to flat surfaces ; a change in flow Reynolds number only slightly changes effectiveness ; a lowering of the mainstream flow Mach number from 0.6 to 0.3 causes a sizable decrease in effectiveness ; a favourable pressure gradient, typical of that seen on a turbine blade also decreases considerably the effectiveness.

7. FUTURE RESEARCH PLANS

Modifications are being planned to measure heat transfer rate at two or more different values of the coolant temperature parameter (by changing both the wall and coolant temperature) in order to provide information on the adiabatic wall temperature and heat transfer coefficient and to check the applicability at variable property flow conditions of the relation

$$q_f = h_f(T_{rm}-T_w)(1-\eta\theta).$$

The experimental data bank of the measurements of film cooling effectiveness under conditions of Mach number, Reynolds number, wall curvature and pressure gradient will be increased allowing improved correlations to be made.

The large hot cascade tunnel CT2, which is now nearing final assembly, will be developed during the second year ready for the third year's program.

REFERENCES

1. GOLDSTEIN R.J. : "Film Cooling", Advances in Heat Transfer, Vol.7, Academic Press, New York, London 1971.

2. LIESS C. : "Film Cooling with Injection from a Row of Inclined Circular Holes - An experimental Study for the Application to Gas Turbine Blades" VKI TN 97, March 1973.

3. JONES T.V., SCHULTZ D.L. : "Film Cooling Studies in Subsonic and Supersonic Flows using a Shock Tunnel" 8th International Shock Tube Symposium, Imperial College, London, July 1971.

4. LOUIS J.F., DERMERJIAN A.M., GOULIOS G.N., TOPPING R.F., WIEDHOPF J.M. : "Short Duration Studies of Turbine Heat Transfer and Film Cooling Effectiveness" ASME 74-GT-131, April 1974.

5. STOLLERY J.L., EL-EHWANY A.A.M. : "A Note on the Use of a Boundary Layer Model for Correlating Film Cooling Data" Int. J. Heat Mass Transfer, Vol.8, 1965, pp.56-65.

6. CHOE H., KAYS W.M., MOFFAT R.J. : "Turbulent Boundary Layer on a Full-Coverage Film-Cooled Surface - An Experimental Heat Transfer Study with Normal Injection" NASA CR-2642, January 1976.

7. METZGER D.E., CANPER H.J. and SWANK L.R. : "Heat Transfer With Film Cooling Near Non-Tangential Injection Slots" ASME Transactions, J.of Eng. Power, 1968, pp. 157-163.

8. METZGER D.E., TAKEUCHI D.I., KUENSTLER O.A. : "Effectiveness and Heat Transfer With Full-Coverage Film Cooling" Trans. ASME J. of Eng. Power, July 1973, pp. 180-184.

9. CRAWFORD M.E., CHOE H., KAYS W.M., MOFFAT R.J. : "Full-Coverage Film Cooling Heat Transfer Study - Summary of Data for Normal-Hole Injection and 30° Slant-Hole Injection" NASA CR-2648, March 1976.

10. SCHULTZ D.L. : "A Survey of Film Cooling Theory and Experiment" VKI L.S. 83, January 1976.

11. LANDER R.D., FISCH R.W., SUO M. : "External Heat Transfer Distribution on Film Cooled Turbine Vanes" J. of Aircraft, Vol.9, No 10, pp. 707-714, October 1972.

12. RICHARDS B.E. : "Heat Transfer to Cooled Turbine Blades - A Review"
VKI L.S. 83, January 1976.

13. LOUIS J.F. : "Short Duration Experimental Techniques in Turbomachines"
VKI L.S. 78, April 1975.

14. JONES T.V., SCHULTZ D.L., HENDLEY A.D. : "On the Flow in an Isentropic Free Piston Tunnel"
ARC R&M 3731, January 1973.

15. RICHARDS B.E. : "Isentropic Light Piston Facilities for Simulation of Hot Flows Through Turbines"
VKI L.S. 78, April 1975.

16. SCHULTZ D.L. and JONES T.V. : "Heat Transfer Measurements in Short Duration Hypersonic Facilities"
AGARDograph 165, 1973.

17. BACKX E. : "The Total Temperature in the Longshot Wind Tunnel - Its Measurement and Evaluation"
VKI TN 98, 1974.

18. SPALDING D.B. and CHI S.W. : "The drag of a compressible turbulent boundary layer on a smooth flat plate with and without heat transfer"
J. Fluid Mech., Vol.18, Pt.1, January 1964, pp.117-143

19. THOMANN H. : "Effect of streamwise wall curvature on heat transfer in a turbulent boundary layer"
J. Fluid Mech., Vol.33, p.283, 1968.

20. BRADSHAW P. "Effects of streamline curvature on turbulent flow"
AGARDograph No 169, August 1973.

TABLE 1 - Test Matrix

Model	M	P_0 bars	T_0 K	Re_{-7} $\times 10^{-7}$	dp/dx mmHg/cm	R mm	m
A	0.6	9.0	522	4.5	0	∞	0.5,1.0,1.5,1.7
B	0.6	9.0	522	4.5	0	130	0.5,1.0,1.5,2.0
C	0.6	9.0	522	4.5	0	65	0.5,1.0,1.5,2.0
A	0.6	8.1	510	4.0	0	∞	0.76, 1.11, 1.31, 1.53, 1.71
A	0.6	3.9	425	2.35	0	∞	0.73, 1.20, 1.47
A	0.3	8.4	510	2.35	0	∞	0.90, 1.50, 2.48
D	0.3 0.6	8.4	510	2.35	170	∞	1.50, 2.11, 2.48 2.87

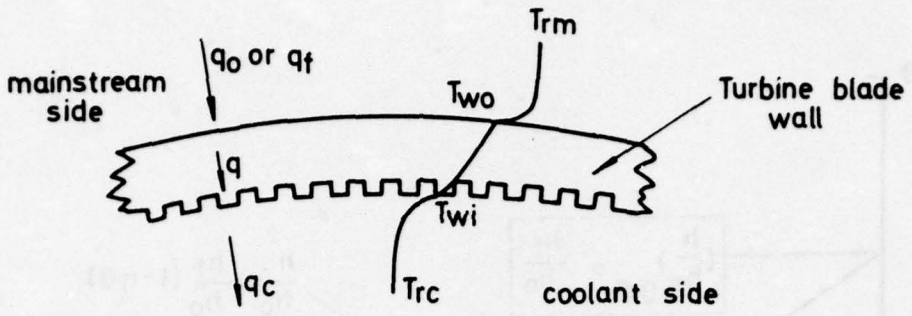

FIG. 1 DESIGN CALCULATION

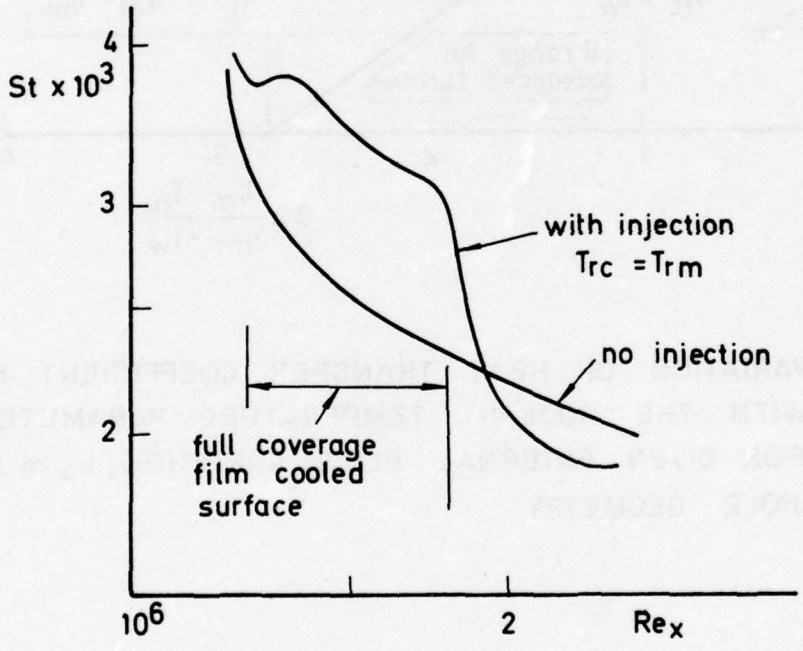

FIG. 2 EFFECT OF COOLANT INJECTION ON NON-DIMENSIONAL HEAT TRANSFER COEFFICIENT

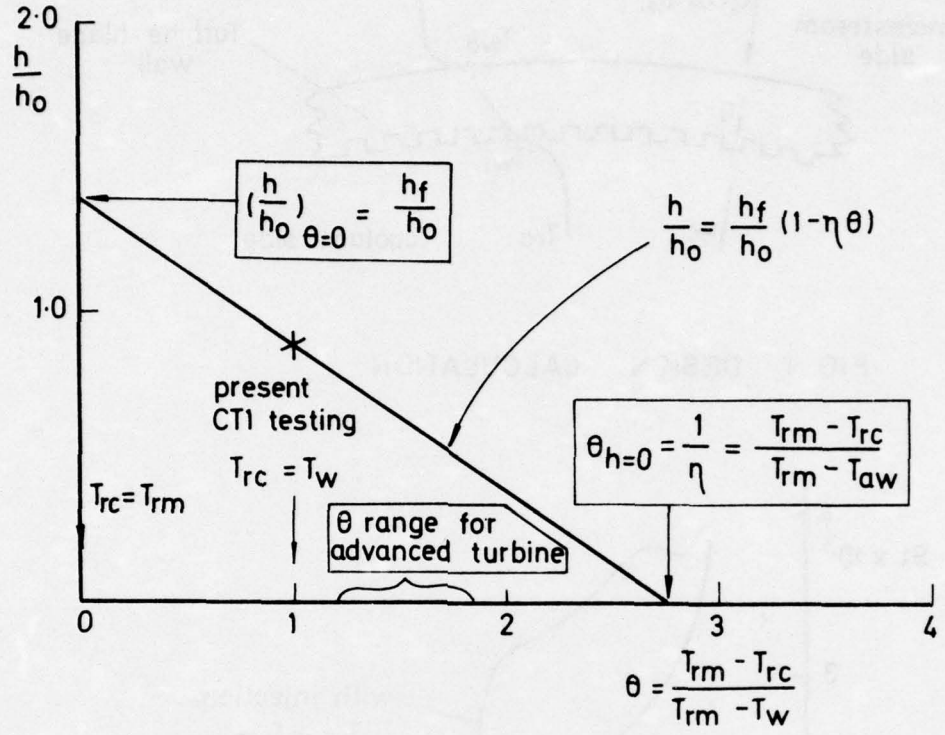

FIG. 3 VARIATION OF HEAT TRANSFER COEFFICIENT, h WITH THE COOLANT TEMPERATURE PARAMETER, θ FOR GIVEN EXTERNAL FLOW CONDITION, x, m AND HOLE GEOMETRY.

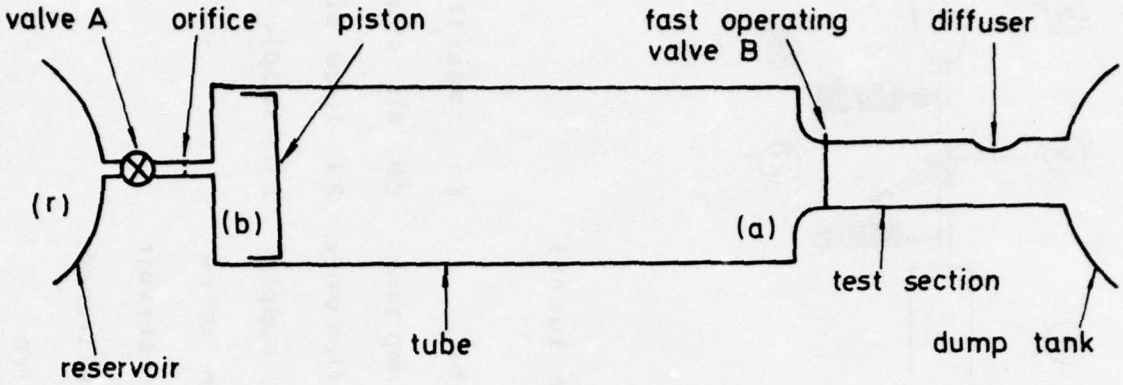

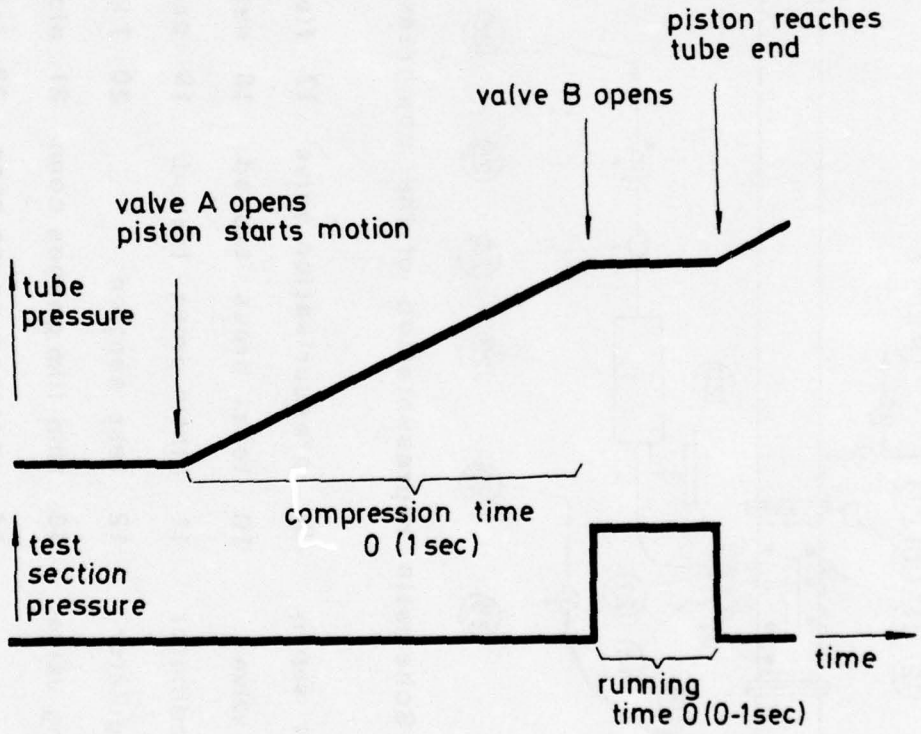

FIG. 4 SCHEMATIC AND OPERATING CYCLE OF ISENTROPIC LIGHT PISTON TUNNEL

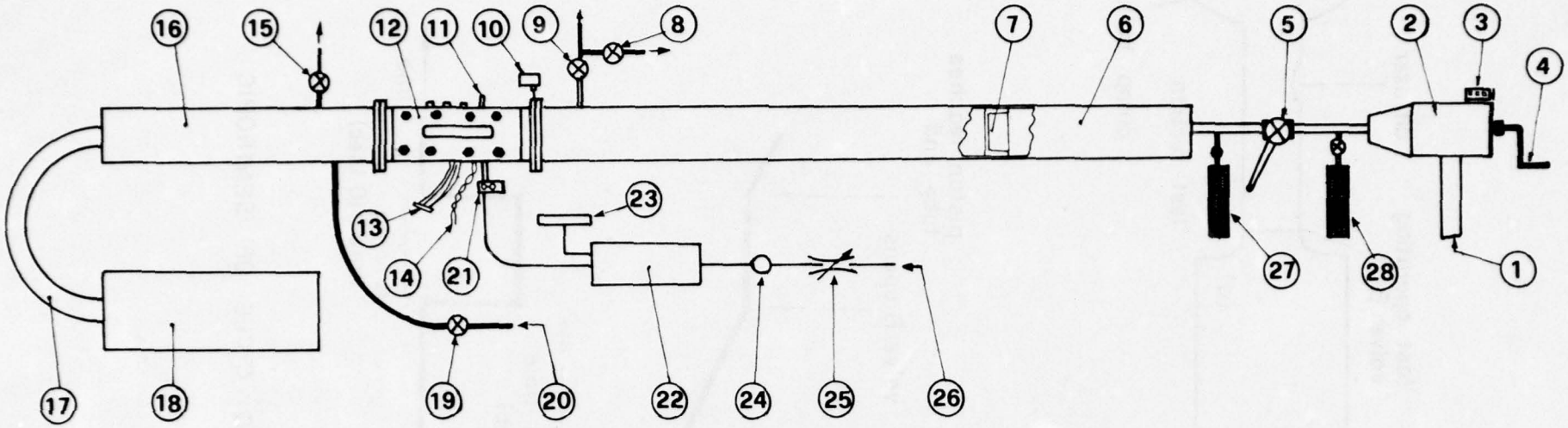

Fig. 5 Schematic representation of the compression tube tunnel

1	40 kg/cm² air supply	9	pressurisation valve	17	flexible tube	25	regulator
2	regulating valve	10	total press. transd.	18	supplem. dump tank	26	air supply
3	position indicator	11	static press. transd.	19	pressurisation valve	27	tube purge
4	opening regulator	12	test section	20	7 kg/cm² air supply	28	supply purge
5	quick opening valve	13	thin film gauges conn.	21	electromagn. valve		
6	tube	14	upstream gauge conn.	22	injection reservoir		
7	piston	15	vaccuum pump valve	23	inject. pres. transd.		
8	relief valve	16	dump tank	24	supply valve		

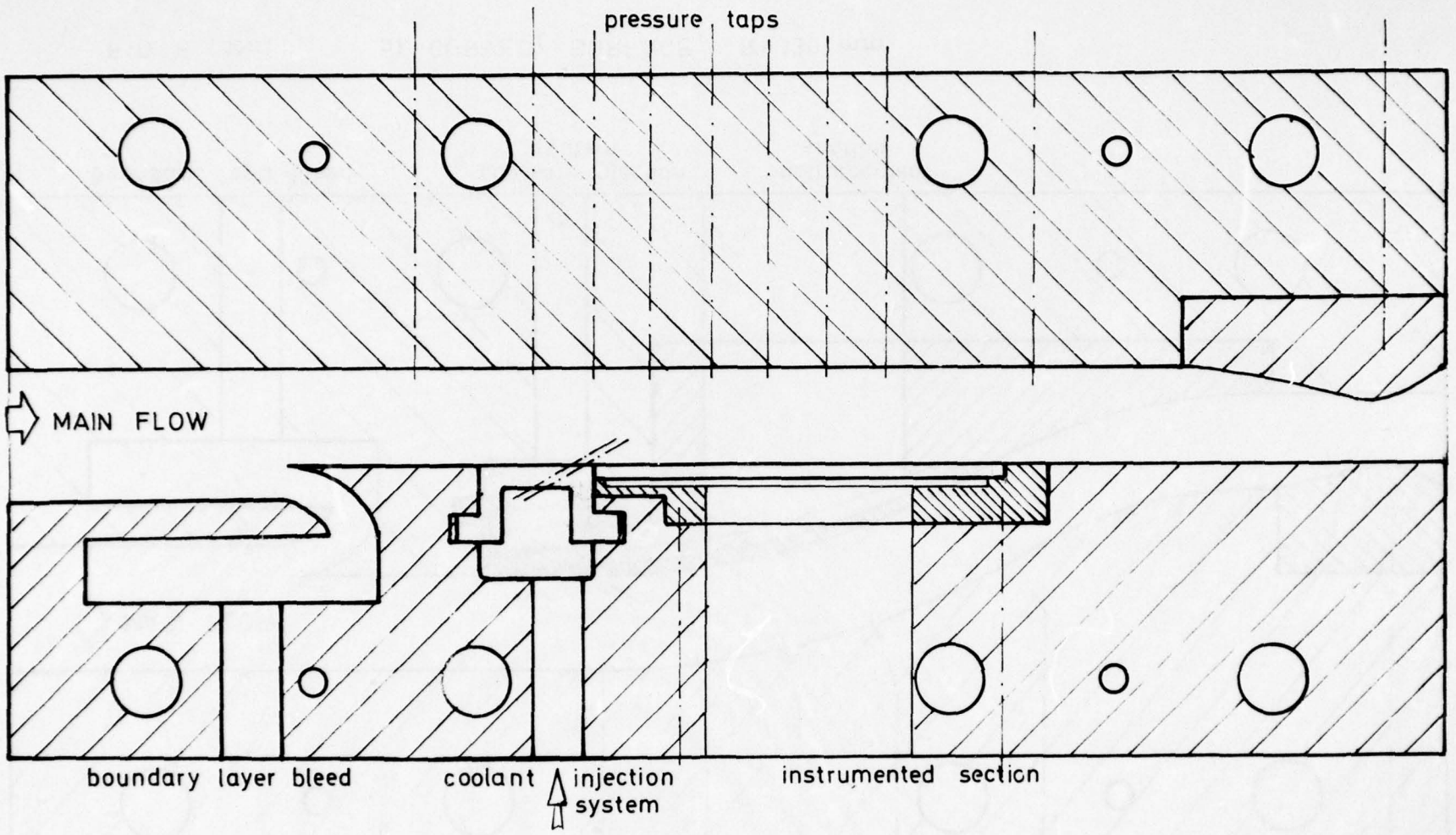

FIG. 6 TEST SECTIONS a) FLAT PLATE - ZERO PRESSURE GRADIENT

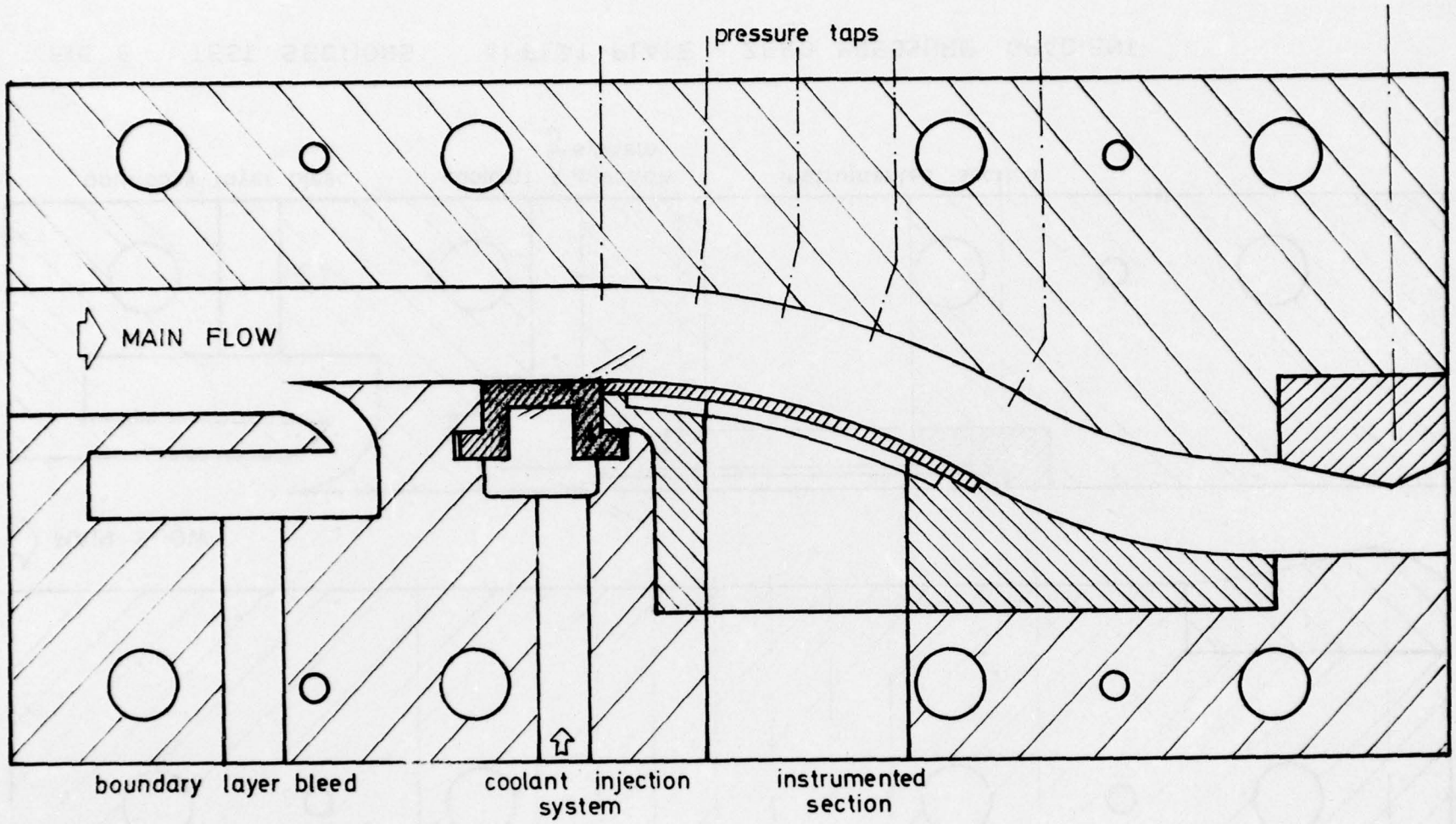

FIG. 6 (cont.) b) CURVED SURFACE, R = 130 mm

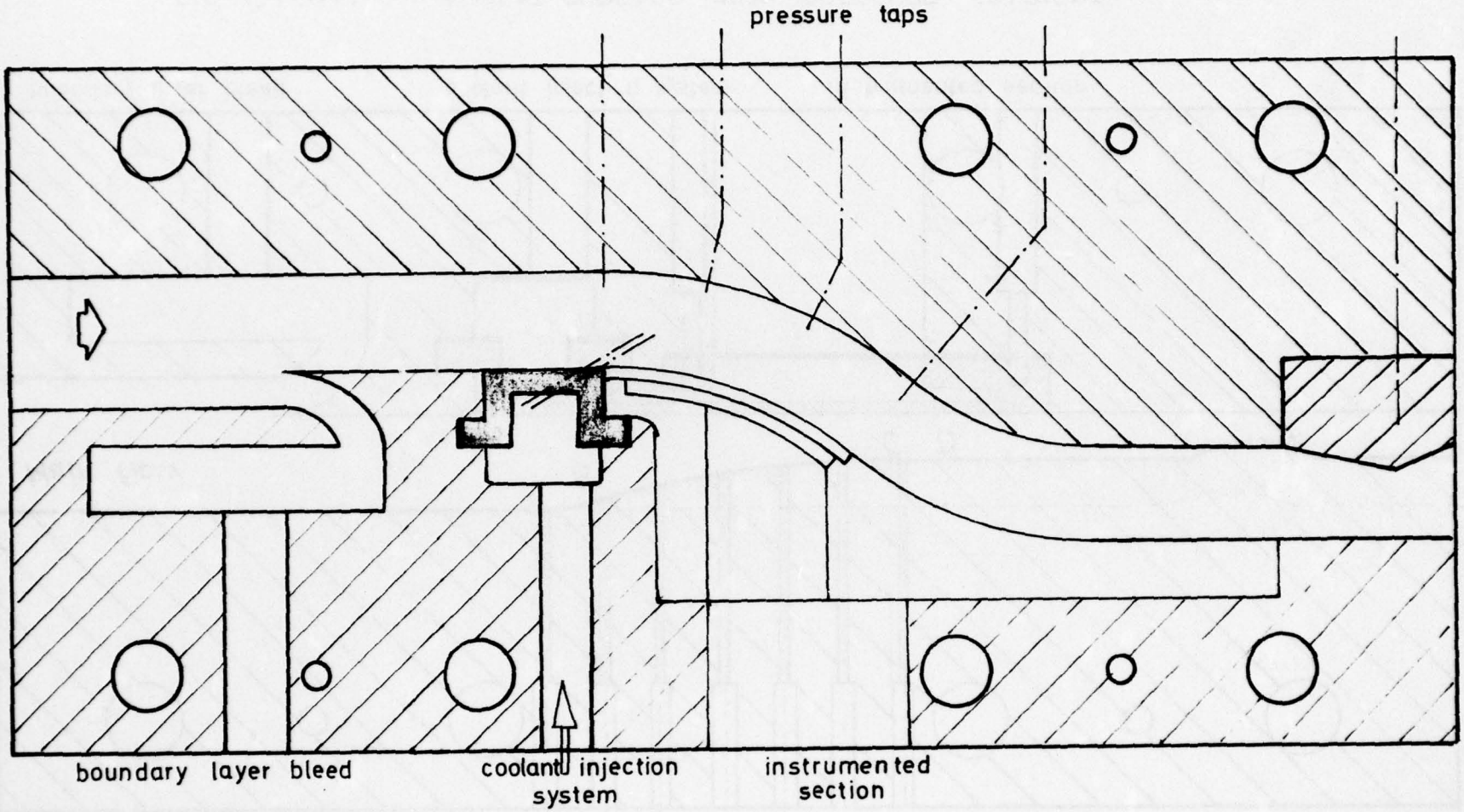

FIG. 6 (cont) c) CURVED SURFACE, R = 65 mm

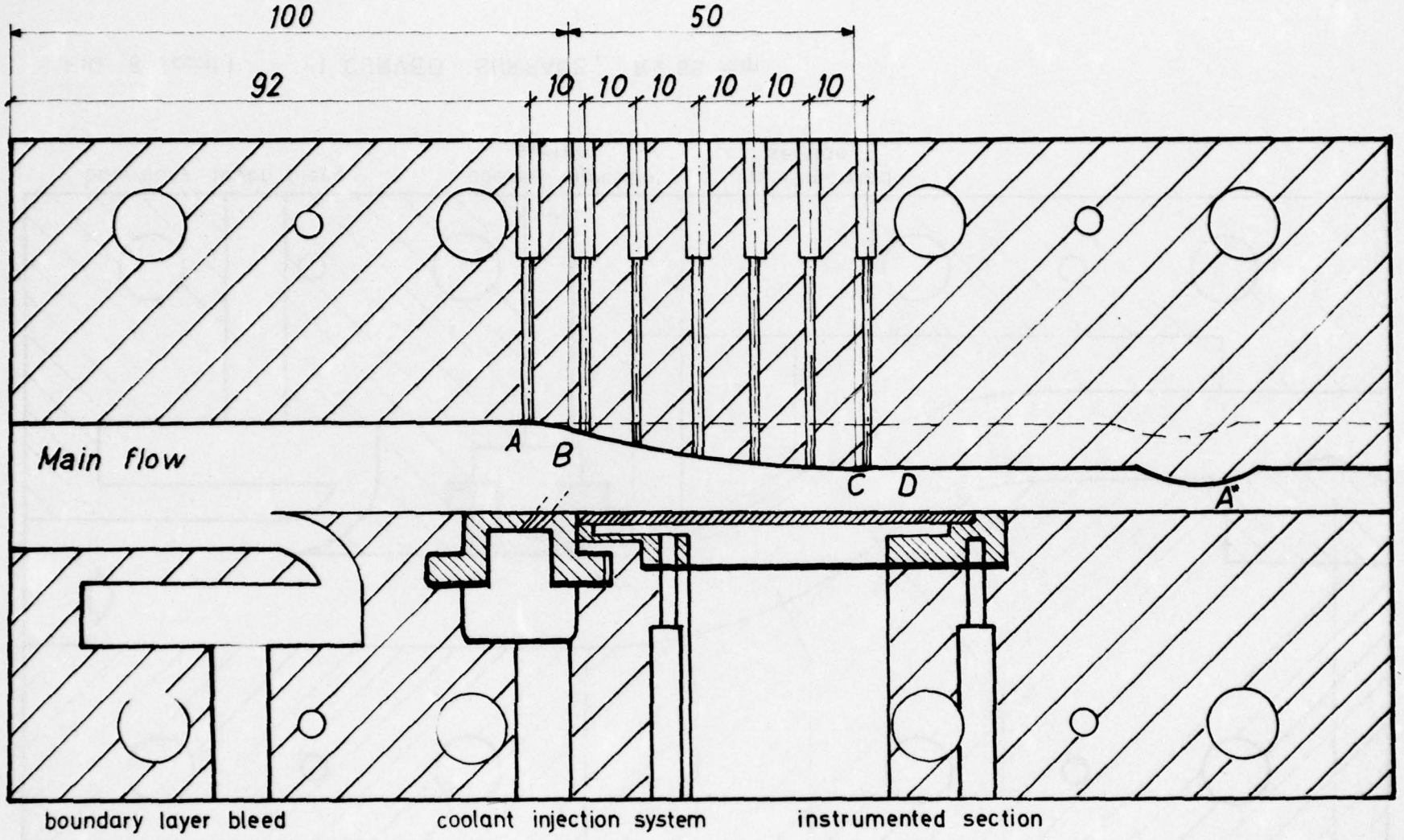

FIG. 6 (cont.) d) FLAT SURFACE WITH PRESSURE GRADIENT

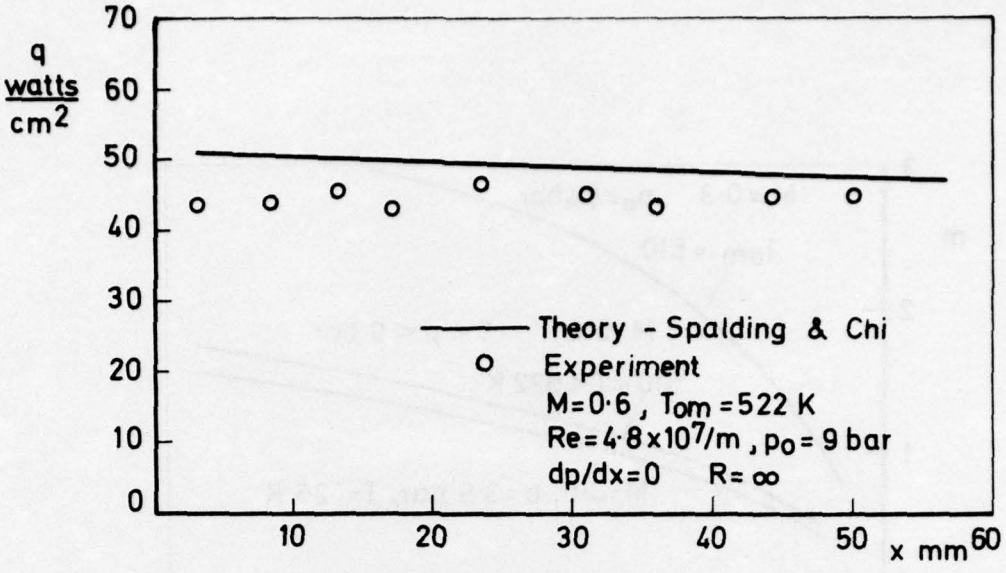

FIG. 7 HEAT TRANSFER DISTRIBUTION ON FLAT PLATE

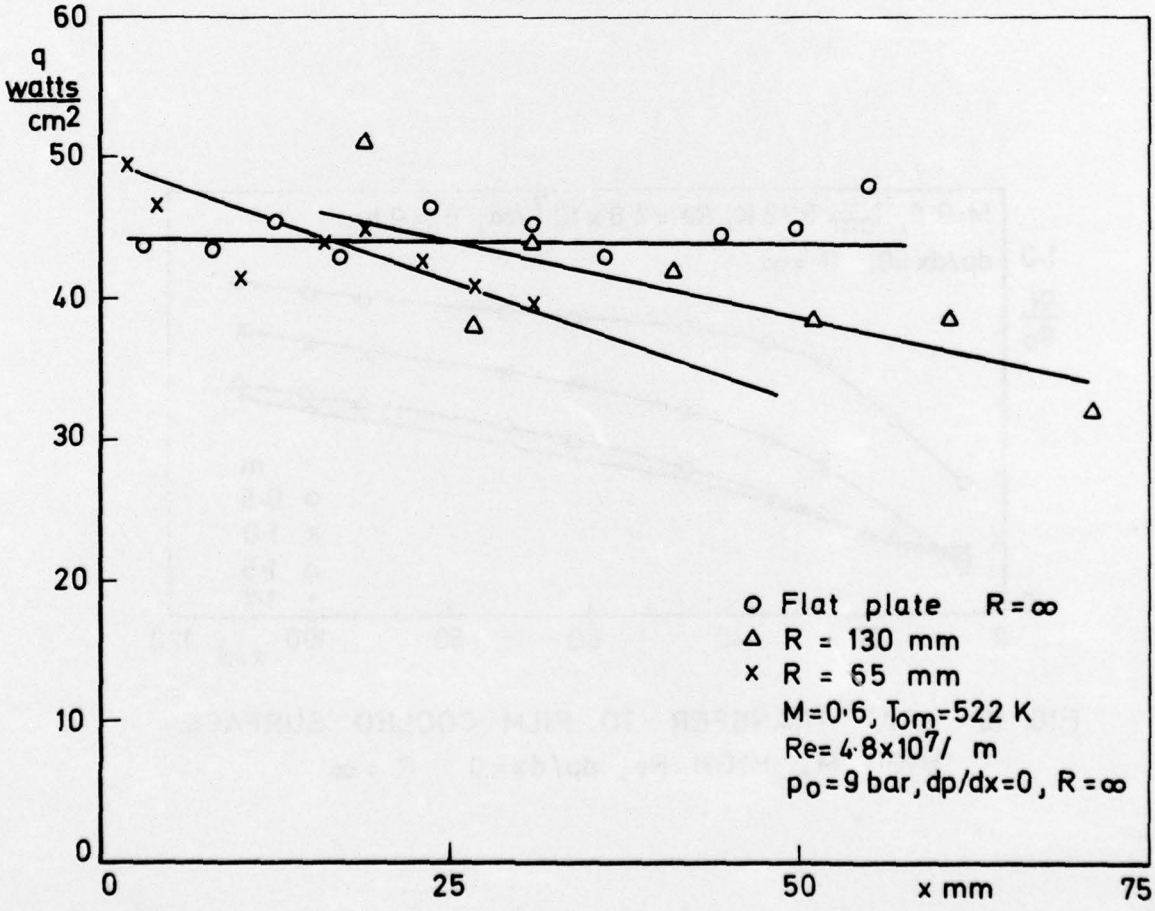

FIG. 8 EFFECT OF SURFACE CURVATURE ON HEAT TRANSFER RATE

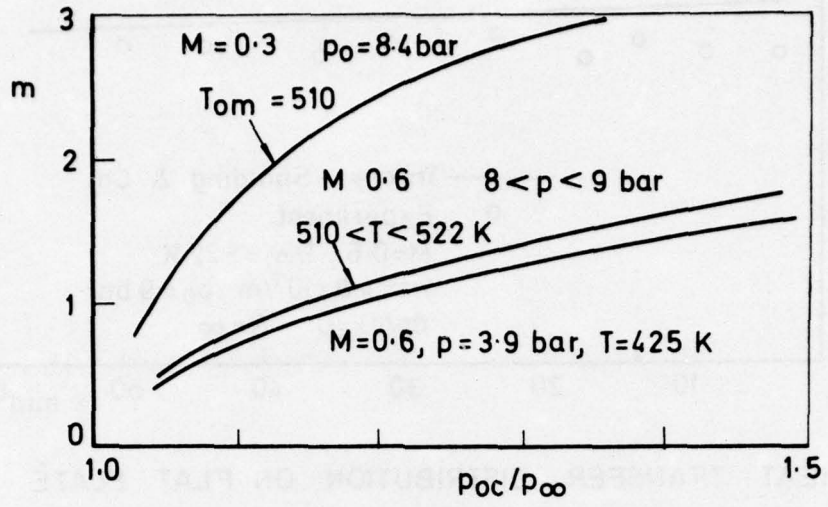

FIG. 9 VARIATION OF COOLANT FLUX PARAMETER, m, WITH COOLANT PRESSURE RATIO

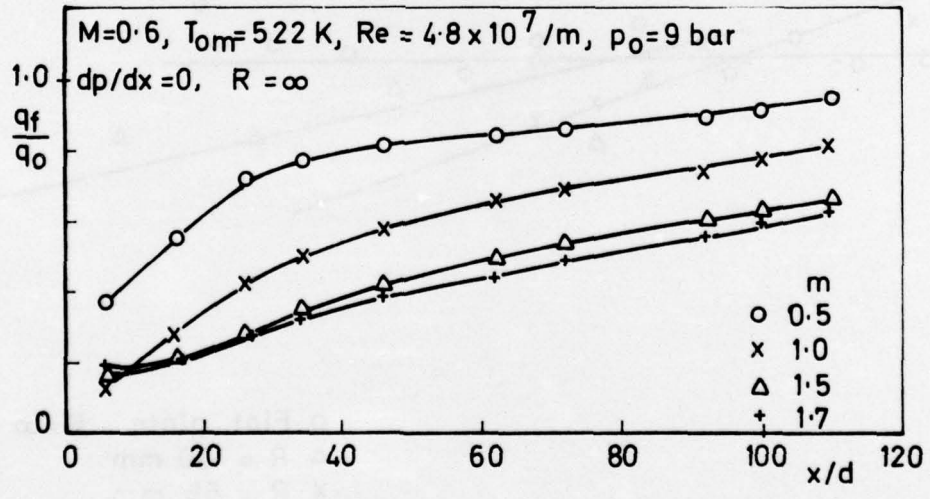

FIG. 10 HEAT TRANSFER TO FILM COOLED SURFACE HIGH M, HIGH Re, dp/dx = 0 R = ∞

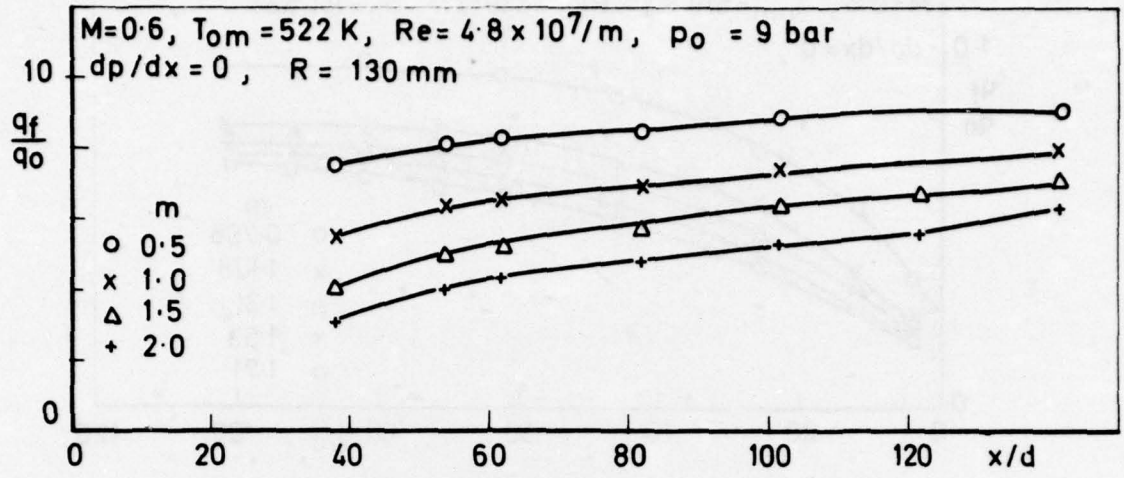

FIG. 11 HEAT TRANSFER TO FILM COOLED SURFACE HIGH M, HIGH Re, dp/dx = 0, R = 130 mm

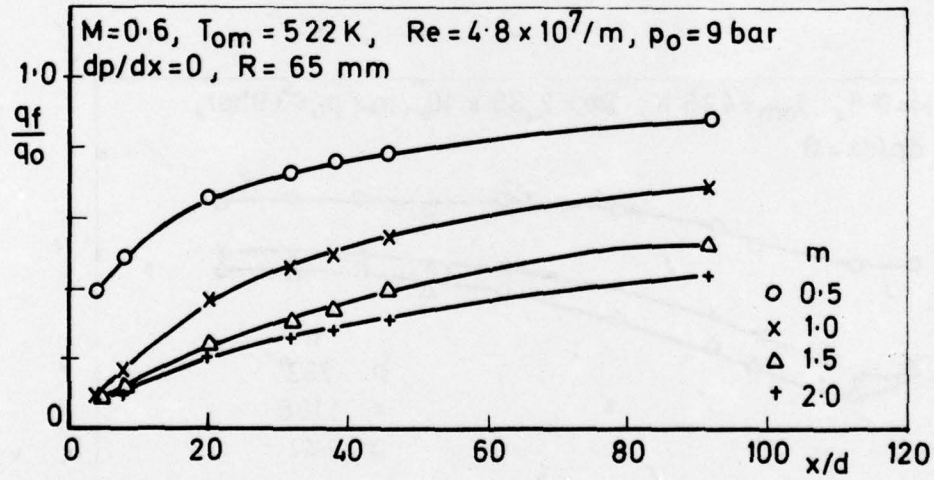

FIG. 12 HEAT TRANSFER TO FILM COOLED SURFACE HIGH M, HIGH Re, dp/dx = 0, R = 65 mm

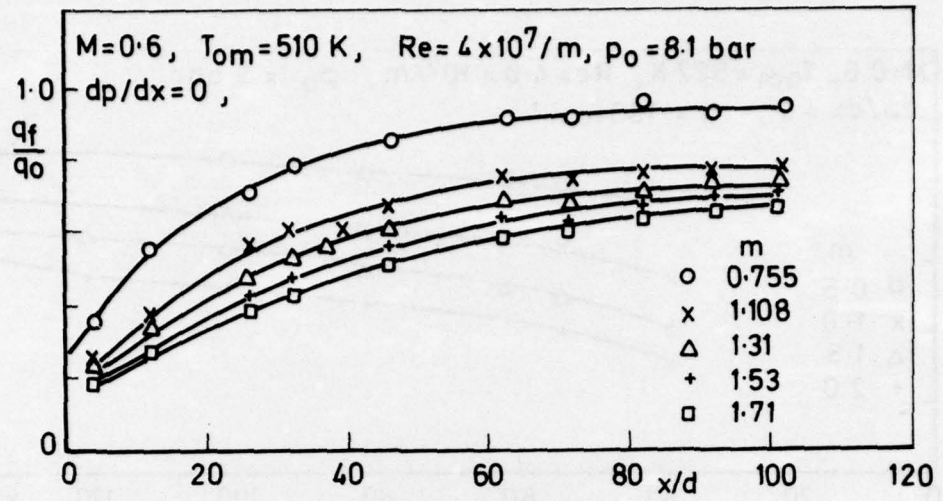

FIG. 13 HEAT TRANSFER TO FILM COOLED SURFACE
HIGH M, HIGH Re, dp/dx = 0, R = ∞

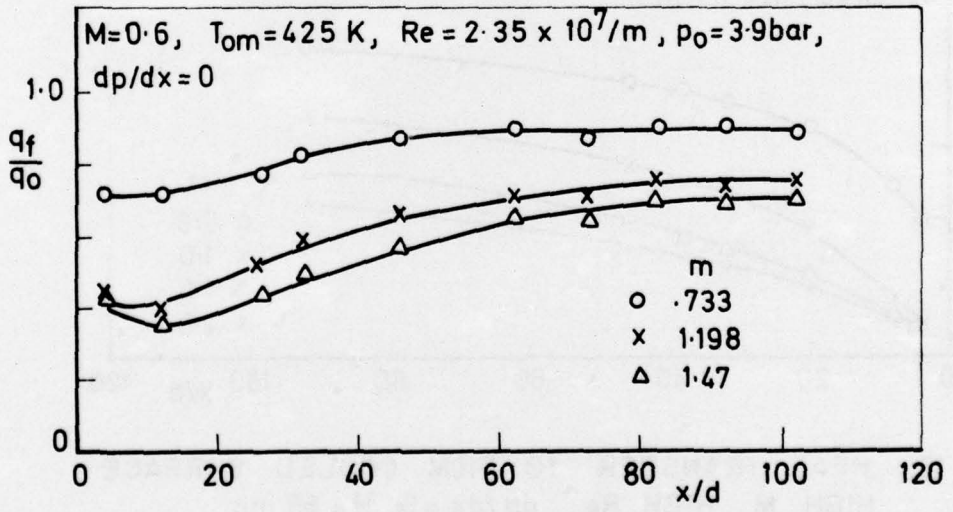

FIG. 14 HEAT TRANSFER TO FILM COOLED SURFACE
HIGH M, LOW Re, dp/dx = 0, R = ∞

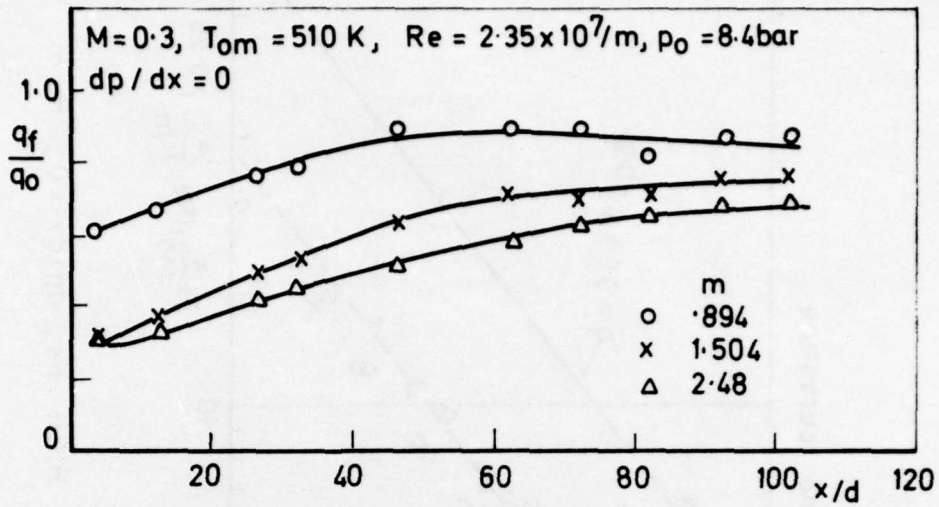

FIG. 15 HEAT TRANSFER TO FILM COOLED SURFACE
LOW M, LOW Re, dp/dx = 0 , R = ∞

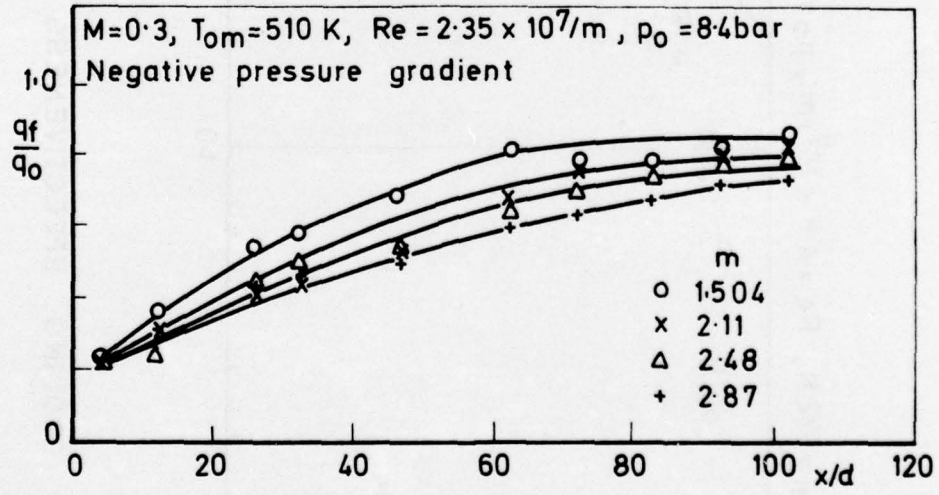

FIG. 16 HEAT TRANSFER TO FILM COOLED SURFACE
LOW M, LOW Re, dp/dx = -ve, R = ∞

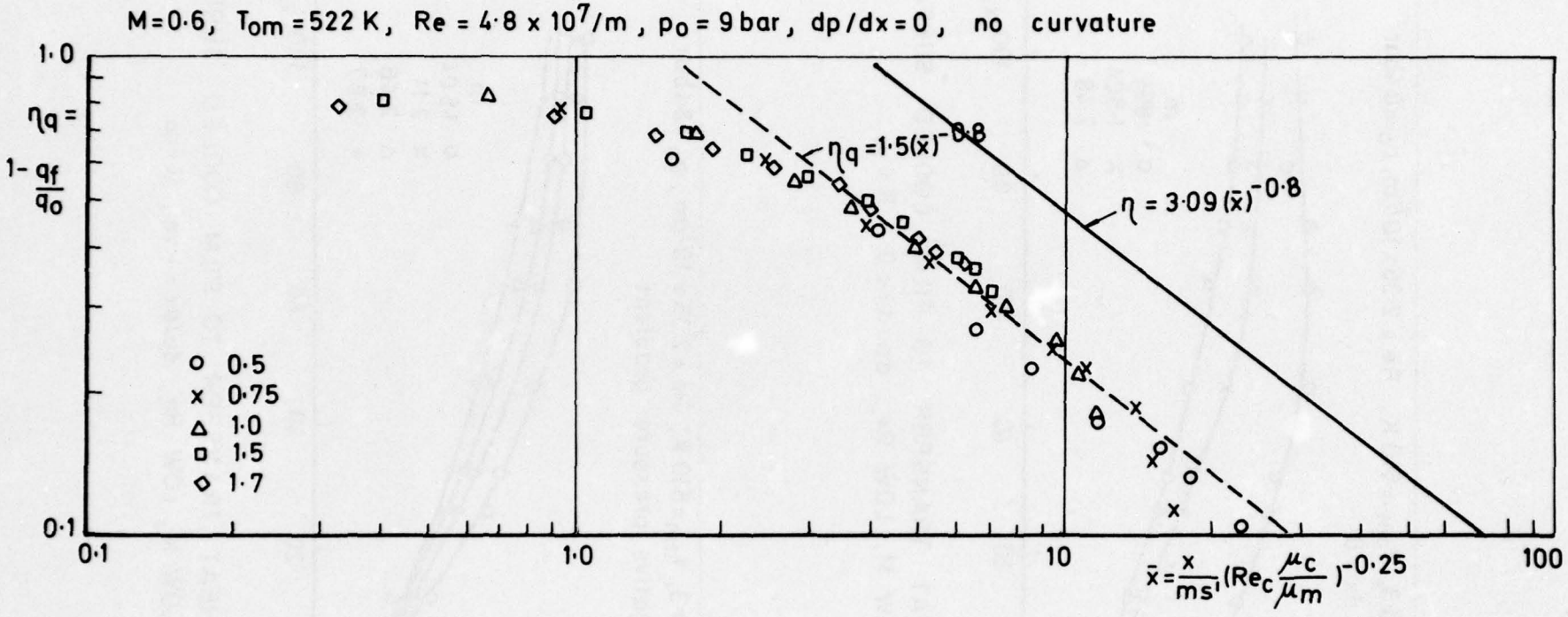

FIG. 17 FILM COOLING EFFECTIVENESS vs. $\bar{x}$. HIGH M, HIGH Re, dp/dx = 0, R = ∞

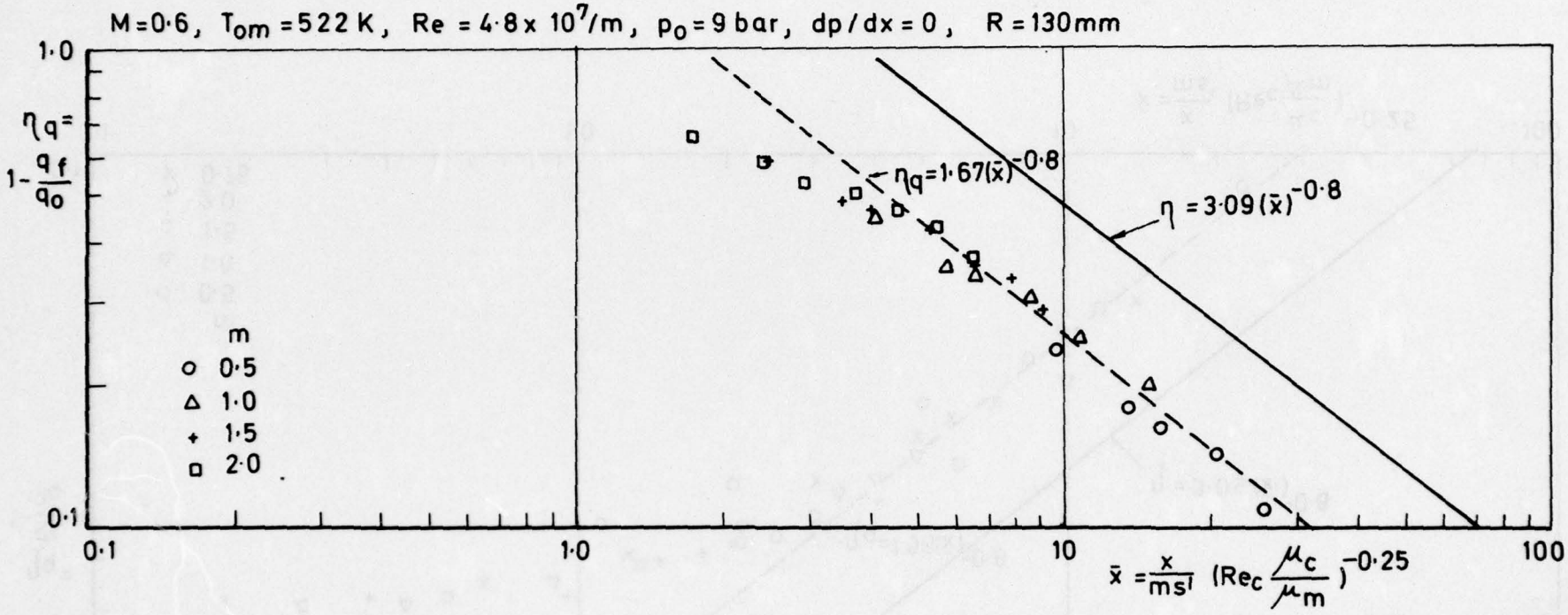

FIG. 18 FILM COOLING EFFECTIVENESS vs. $\bar{x}$. HIGH M, HIGH Re, dp/dx = 0, R = 130 mm

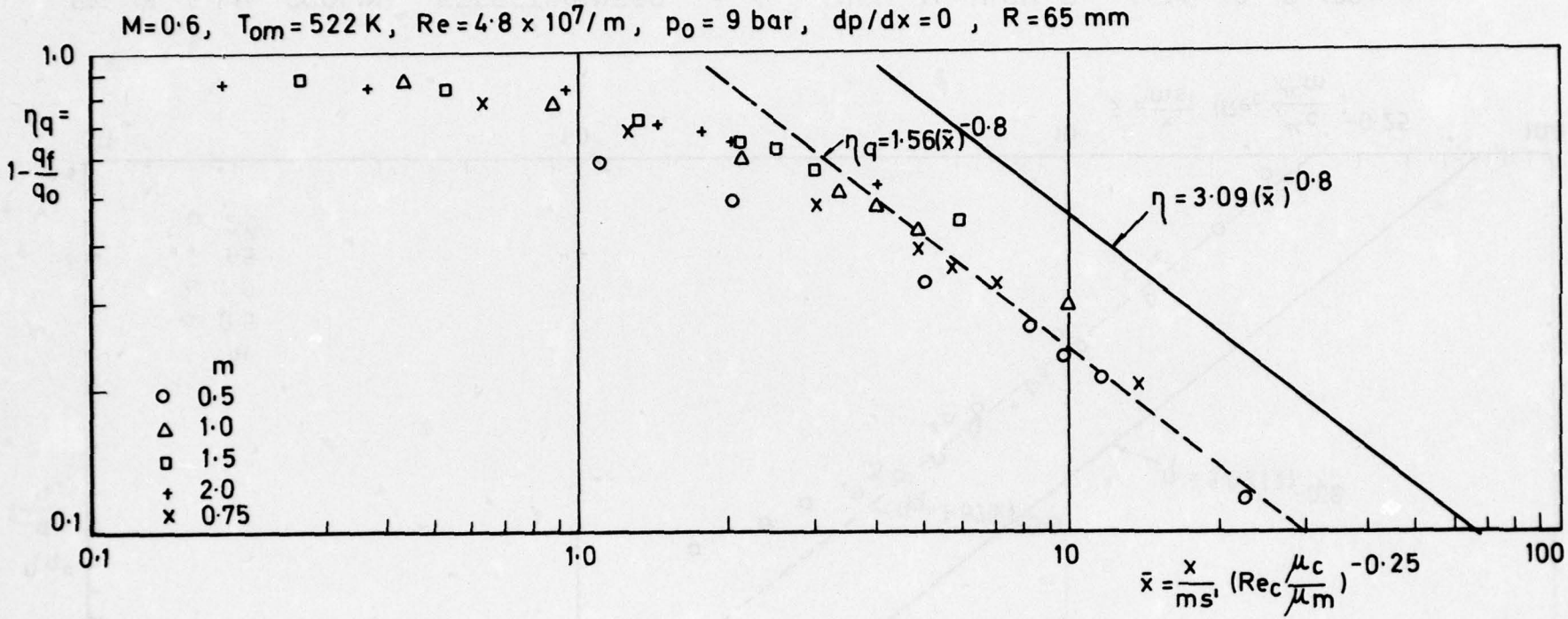

FIG. 19 FILM COOLING EFFECTIVENESS vs. $\bar{x}$. HIGH M, HIGH Re, dp/dx = 0, R = 65 mm

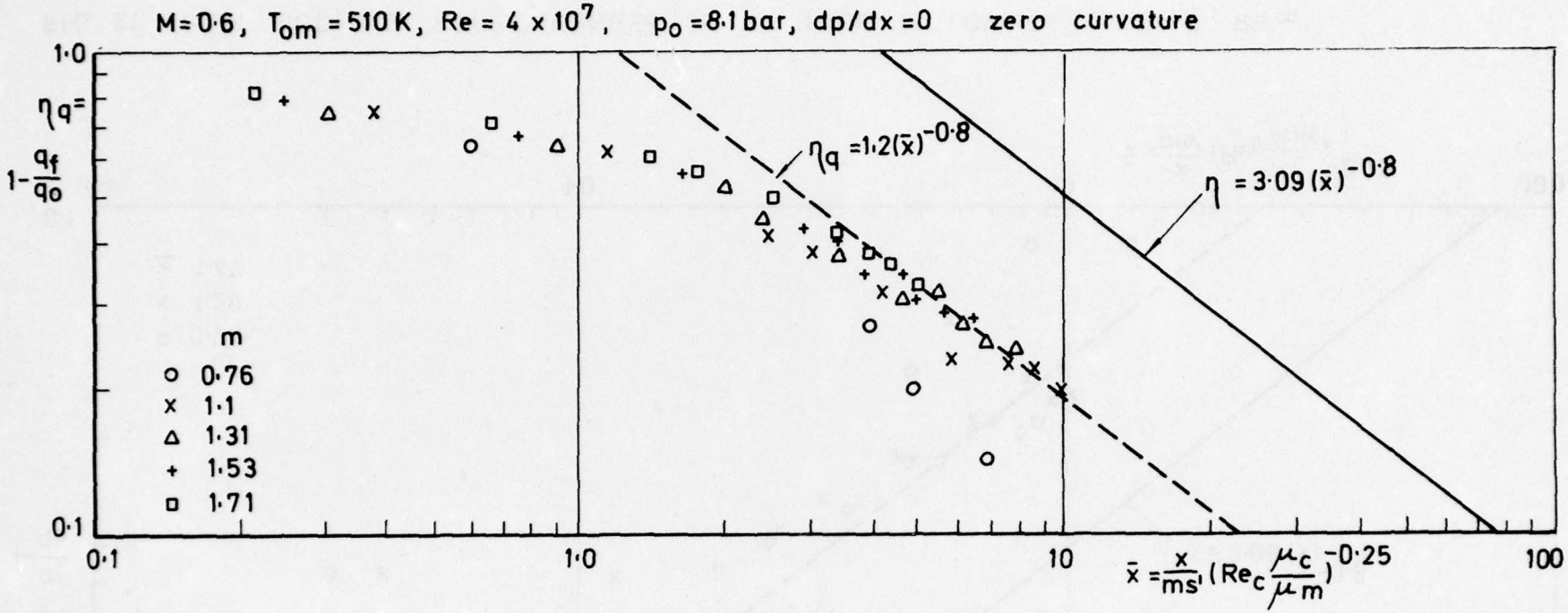

FIG. 20 FILM COOLING EFFECTIVENESS vs. $\bar{x}$ HIGH M, HIGH Re, dp/dx = 0, R = ∞

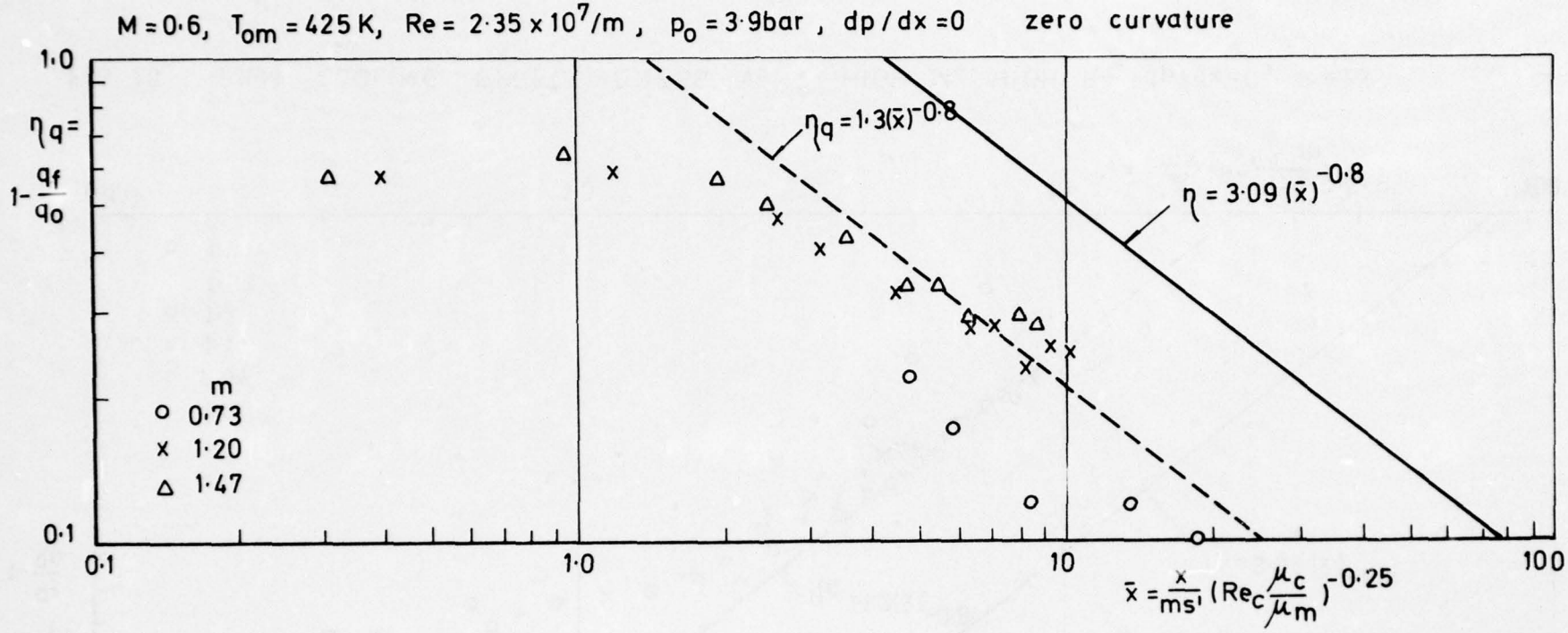

FIG. 21 FILM COOLING EFFECTIVENESS vs. $\bar{x}$. HIGH M, LOW Re, dp/dx = 0 , R = ∞

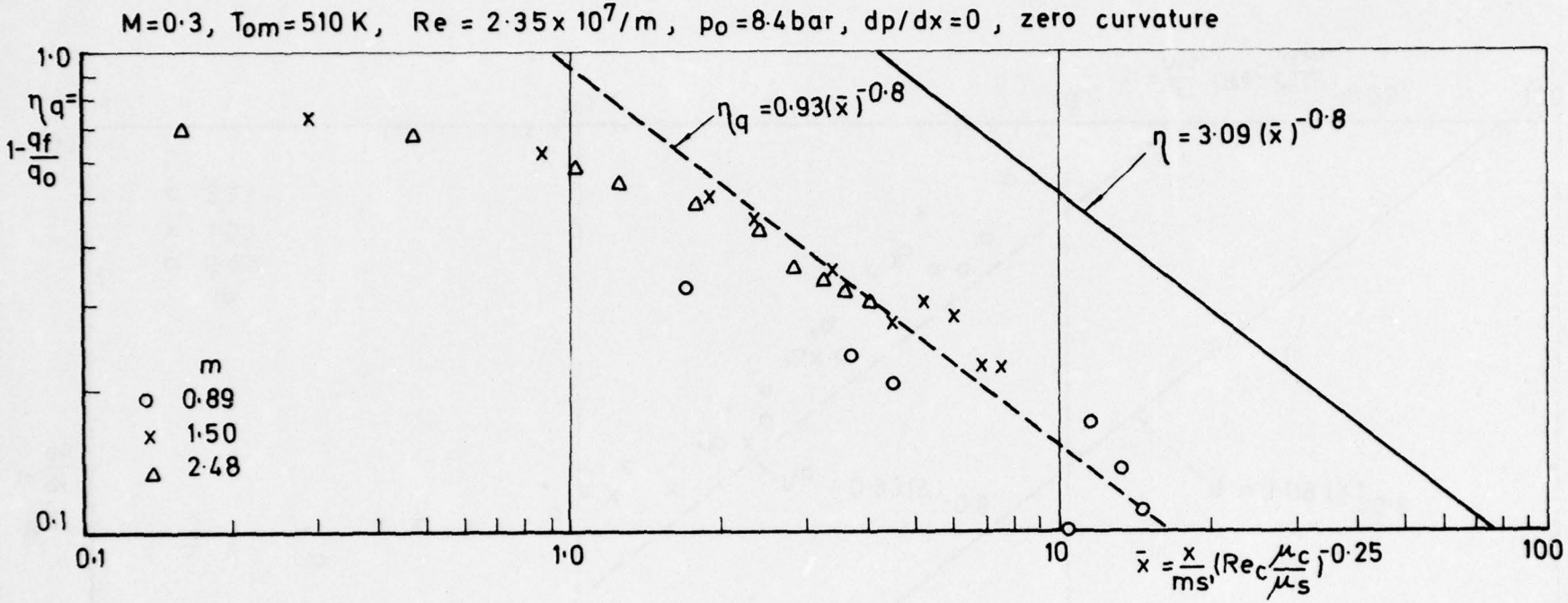

FIG. 22 FILM COOLING PARAMETER vs. $\bar{x}$. LOW M, LOW Re, dp/dx = 0, R = ∞

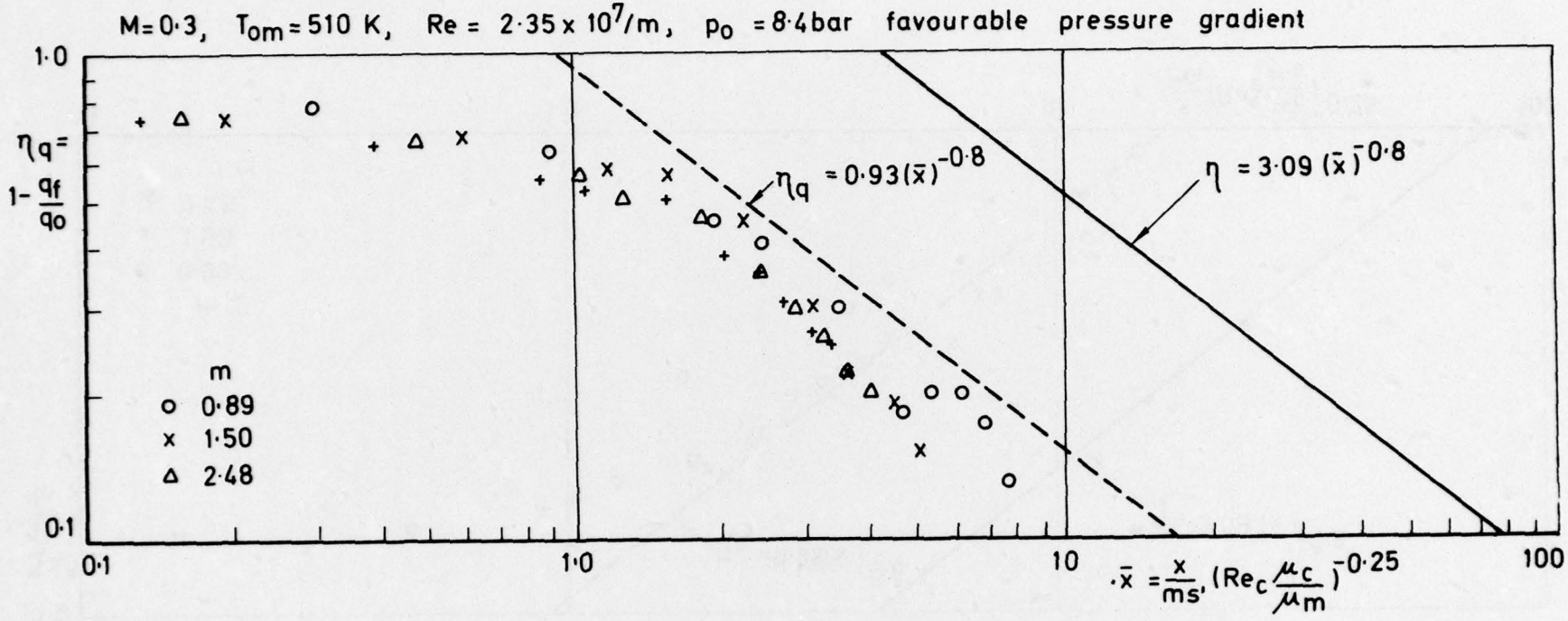

FIG. 23 FILM COOLING EFFECTIVENESS VS. $\bar{x}$. LOW M, LOW Re, dp/dx = -ve, R = ∞